Organic–Inorganic Hybrid Interfaces for Spin Injection into Carbon Nanotubes and Graphene

Pascal Martin, Bruno Dlubak, Pierre Seneor, Richard Mattana, Marie-blandine Martin, Philippe Lafarge, François Mallet, Maria Luisa Della Rocca, Simon M.-m. Dubois, Jean-christophe Charlier, et al.

ADVANCED QUANTUM TECHNOLOGIES
www.advquantumtech.com

Organic–Inorganic Hybrid Interfaces for Spin Injection into Carbon Nanotubes and Graphene

Pascal Martin, Bruno Dlubak, Pierre Seneor, Richard Mattana, Marie-Blandine Martin, Philippe Lafarge, François Mallet, Maria Luisa Della Rocca, Simon M.-M. Dubois, Jean-Christophe Charlier, and Clément Barraud**

Spintronics is a quantum technology which aims at adding the spin quantum degree of freedom to conventional CMOS electronics. Since the discovery of the giant magneto-resistance in 1988, considered as the birth of this field, spintronics continues flooding the market with plethora of devices used in everyday life applications such as hard drive read heads or magnetic random-access memories, and so on. From a fundamental research perspective, the field is still blooming bringing post-CMOS perspectives technologically closer to the reality with, for instance, prototypes of all-spin-logic circuits and neuromorphic chips. To sustain this intense research activity, a quest for new platform materials is also taking place not only to enhance existing performances but also to generate novel functionalities. In this vein, carbon nanostructures such as molecules, graphene, and carbon nanotubes are among the most sought-after materials. In this review, spin transport experiments in carbon nanotubes and graphene are first detailed and then, the necessity to consider new hybrid interfaces are highlighted for a better control of the spin injection at the quantum device level.

1. Introduction

Spin electronics or spintronics[1,2] is a quantum technology which aims at adding the spin quantum degree of freedom to conventional CMOS electronics. Since the discovery of the giant magneto-resistance (GMR) in ultrathin Fe/Cr multilayers in 1988 independently by the groups of Fert[3] and Grünberg,[4] considered as the birth of this field,[5] spintronics continues flooding the market with plethora of devices used in everyday life applications such as hard drive read heads, magnetic random-access memories or ultrasensitive magnetic sensors.[6] From a fundamental research perspective, the field is still blooming bringing post-CMOS perspectives technologically closer to the reality with, for instance, prototypes of all-spin-logic circuits[7,8] and neuromorphic chips.[9,10] To sustain this intense research activity, a quest for new platform materials is also taking place not only to enhance existing performances but also to generate novel functionalities.[11] In this vein, carbon nanostructures such as molecules, graphene, and carbon nanotubes are among the most sought-after materials.[12–14] The reason can be given by considering a core requirement of spin electronics: the spin information needs to be conserved during a spintronics device operation until it is manipulated for computations. Spin information storage is achieved in hard magnetic materials with a more and more reduced numbers of individual spins.[15] However, transporting spins in a non-magnetic material over long distances (>100 μm) between two gates[16] remains a great technological lock. Indeed, it is mainly attributed to two phenomena with quantum origins:

1) The spin-based information is fragile by essence and can be easily lost by different processes within the host material.[17] Conducting or semiconducting materials presenting weak spin scattering are thus interesting.[18]
2) The spin injection process is particularly inefficient between materials of different electronic natures (i.e., from a metal to a semiconductor for instance)[19,20] and a careful investigation and tuning of the interfacial spin dependent transmission is needed. More specifically, an intercalated barrier with well-calibrated properties is generally needed between the spin

P. Martin
Laboratoire ITODYS
CNRS
Université de Paris
UMR 7086 rue Jean Antoine de Baïf 15, Paris 75013, France
B. Dlubak, P. Seneor, R. Mattana, M.-B. Martin
Unité Mixte de Physique
CNRS
Thales
Université Paris-Saclay
avenue Augustin Fresnel 1, Palaiseau 91767, France
E-mail: bruno.dlubak@cnrs-thales.fr
P. Lafarge, F. Mallet, M. L. Della Rocca, C. Barraud
Laboratoire Matériaux et Phénomènes Quantiques
CNRS
Université de Paris
UMR 7162 rue Alice Domon et Léonie Duquet 10, Paris 75013, France
E-mail: clement.barraud@univ-paris-diderot.fr
S. M.-M. Dubois, J.-C. Charlier
Institute of Condensed Matter and Nanosciences (IMCN)
Université catholique de Louvain (UCL)
Chemin des étoiles 8, Louvain-la-Neuve 1348, Belgium

The ORCID identification number(s) for the author(s) of this article can be found under https://doi.org/10.1002/qute.202100166

DOI: 10.1002/qute.202100166

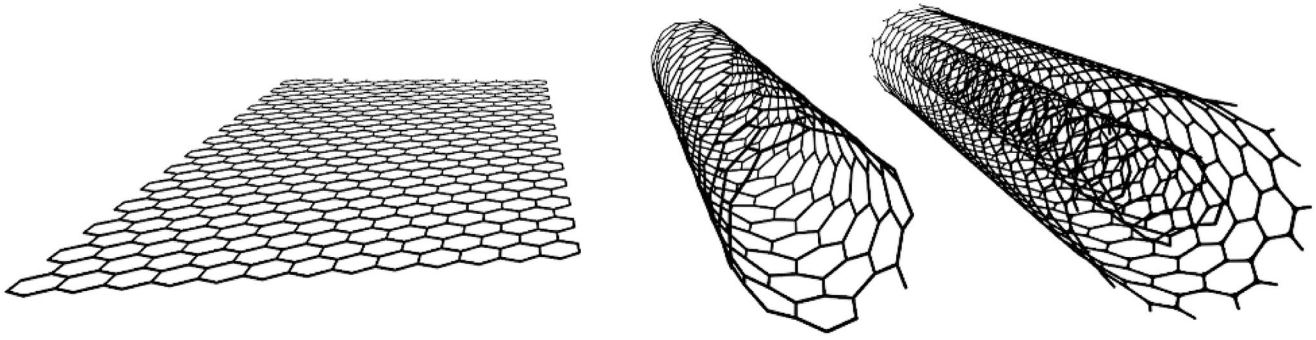

Figure 1. Schematics of a single wall carbon nanotube (SWNT) in the center built by rolling up a graphene nanoribbon (shown on the left). The schematics of a multiwall (double-wall here) carbon nanotube (MWNT) is shown on the right. The outer diameter of a multiwall nanotube can well exceed 50 nm.

source and the propagating channel to enable and efficiently regulate the spin currents.[20–22]

In this review, spin transport experiments in carbon nanotubes and graphene will be first detailed and then, the necessity to consider new hybrid interfaces will be highlighted for a better control of the spin injection at the quantum device level.

2. Carbon Nanotubes and Graphene

Historically, carbon nanotubes were discovered in 1991 by Iijima at the NEC laboratory in Japan.[23] They are 1D tubular nanoscopic structures uniquely composed of C atoms arranged in a honeycomb lattice rolled-up to form a tube with diameter ranging from 0.5 nm to several tenths of nm. Starting from a graphene nanoribbon, a quasi-1D stripe of graphene, the crystal structures of a single wall carbon nanotube (SWNT) and a multiwall carbon nanotube (MWNT) are depicted in **Figure 1** in the center and right of the image respectively. Graphene was discovered later in 2004 by Geim and Novoselov at the University of Manchester.[24]

Today with the discovery of unconventional superconducting[25,26] or ferromagnetic[27] phases in 2D moiré or the exploration of light emission properties of carbon nanotubes[28] or transport properties of 1D moiré,[29,30] those nanomaterials continue to reveal novel physics at the fundamental level[15] but also starts to find a path toward applications such as touch screens.[31] Their unique quantum properties in terms of electronic and optical applications are fully detailed in the following reviews.[32–34]

In this review, we will focus more on the application of such carbon-based nanomaterials to spintronics and we will stress the importance to properly consider the different interfaces at play. The original interest from the spintronics community toward such π-conjugated carbon-based nanomaterials originates from two complementary aspects:

1) The expected extremely long spin lifetimes due to weak spin-orbit coupling of light chemical elements such as C and to the weak hyperfine interactions of π-conjugated systems insensitive to nuclear spins.[18] Past measurements in molecular compounds revealed spin lifetimes exceeding 10 μs[35,36] against 0.1–1 ns in semiconductors[35] and 1 and 100 ps in metals.[37]
2) The rather large Fermi velocity of charge carrier moving through graphene and nanotubes ($v_F = 8 \times 10^5$ m s^{-1}) generally associated to long elastic mean free paths up to 28 μm in graphene for instance[32,38] against 1–30 nm in standard metals.[39]

Playing in concert, those two specific features, characterizing both carbon nanotubes and graphene, bring expectations for large spin diffusion lengths well-beyond the micrometer range as usually found in inorganic semiconductors like Si.[14,40] In this review, we will first describe the pioneering spin transport experiments performed in single-wall and multiwall carbon nanotubes and in graphene. We will emphasize the lack of control or the wrong calibration regarding spin injection/detection properties usually pointed out as the large dispersion presented in the literature in the contact resistance between a spin source and the transport channel being a carbon nanotube or graphene. We will show how this extrinsically limits spin transport properties of those promising systems. We will then discuss the benefits of hybrid organic barriers for spin injection in carbon-based channels, such as nanotubes and graphene, unlocking giant spin signals.

3. Physics of Lateral Spin-Valves

In their simplest form, the studied devices present a unique lateral architecture depicted on **Figure 2**a: two ferromagnetic electrodes with colinear magnetizations (in blue) with two tunnel contacts (in black) separated by a conducting or semiconducting channel (in gray) with a certain length (L) constituted by the carbon nanomaterial (i.e., graphene or carbon nanotube). The first and second electrodes act as a spin polarizer and a spin analyzer, respectively. Both polarizer and analyzer are characterized by a specific spin polarization (P_i). The spin polarization P_i quantify the imbalance between the two spin directions of the injected/detected charge current $J = J_i^{\uparrow} + J_i^{\downarrow}$. In a magnetic tunnel junction (shown in Figure 2b) it can also be defined in terms of the effective tunneling density of states $D_i^{\uparrow\downarrow}$[41]

$$P_i = \frac{J_i^{\uparrow} - J_i^{\downarrow}}{J_i^{\uparrow} + J_i^{\downarrow}} = \frac{D_i^{\uparrow} - D_i^{\downarrow}}{D_i^{\uparrow} + D_i^{\downarrow}} \quad (1)$$

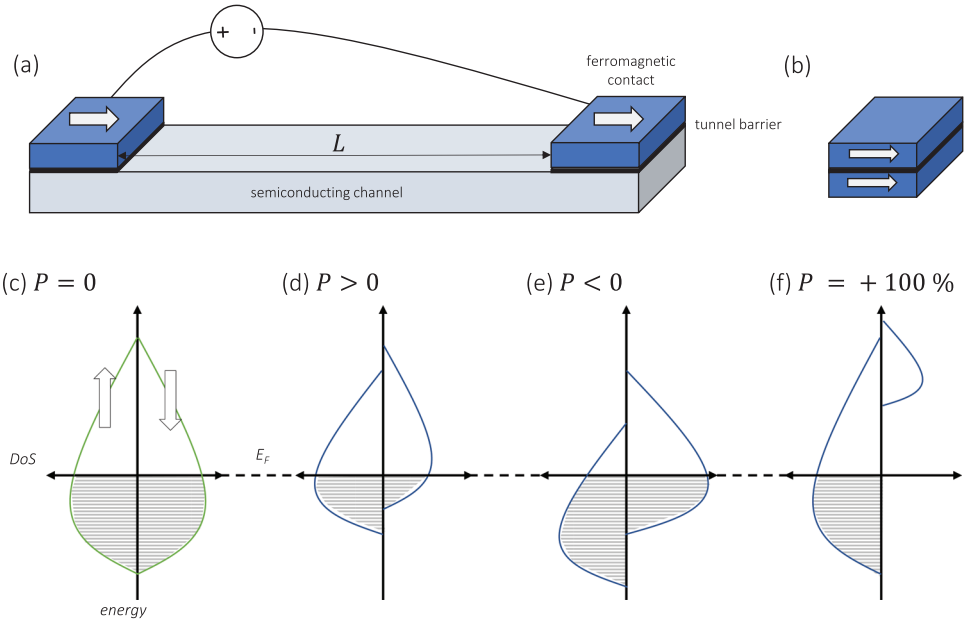

Figure 2. a) Schematic of a lateral spin-valve architecture with two electrodes (in blue) composed of a ferromagnetic metal and a thin tunnel barrier (in black) separated by a semiconducting channel (in light blue). b) Schematic of a magnetic tunnel junction with two electrodes (in blue) composed of a ferromagnetic metal separated by an ultrathin (<3 nm) tunnel barrier (in black). Schematics of the density of states for c) a non-magnetic metal ($P = 0$), a ferromagnetic metal, d) positively spin polarized ($P > 0$), e) negatively spin polarized ($P < 0$), and f) fully spin polarized ($P = +100\%$).

$P_i = 0$ (Figure 2c) means for instance that the two spin directions are equally injected. $P_i = 1$ (Figure 2f) means on the contrary that only one spin direction is injected. It can present a negative sign if the majority spin (noted ↑) direction is less injected than the minority spin direction (noted ↓) at a given energy as shown in Figure 2d,e. Note that, by convention, the majority spin direction identifies the most important spin population ($N^{\uparrow}$) within the ferromagnetic material expressed by

$$N^{\uparrow} = e\int_0^{E_F} \rho(\epsilon)^{\uparrow} d\epsilon > N^{\downarrow} = e\int_0^{E_F} \rho(\epsilon)^{\downarrow} d\epsilon \quad (2)$$

where, $\rho(\epsilon)^{\uparrow\downarrow}$ designates the spin resolved density of states.

The effective tunneling density of states and, a fortiori, the spin polarization is energy dependent quantities. In the free electron model, at equilibrium, and in the limit of a high tunneling barrier, it is reasonable to associate $D_i^{\uparrow\downarrow}$ with the spin-resolved Fermi level density of states.[41] In a real spin polarizer/analyzer, the situation is more complex as each state has a different probability to tunnel through the barrier and to overlap with a propagating state of the channel. For example, it has been recognized early on that, states of s and p characters dominate the tunneling current from transition metal ferromagnets even though d-like electrons contribute predominantly to the Fermi level density of states.[42–44] In these cases, the estimation of $D_i^{\uparrow\downarrow}$ from the total density of states would lead to a predicted negative polarization, while the spin polarization observed experimentally has just the opposite sign[45] at least with standard Al_2O_3 and MgO barriers.[41,46]

As a consequence, the calculation of the Fermi level density of states of the ferromagnet, routinely computed in the framework of density functional theory (DFT),[47,48] is not sufficient to a priori estimate the spin polarization. Indeed, in the calculation of D_i, each electronic state has to be suitably weighted to account for its ability to tunnel through the barrier and to overlap with an electronic state of the channel. In the case of tunneling from a ferromagnet through an epitaxial barrier, qualitative conclusions regarding the sign and magnitude of P_i can be drawn from the symmetries of the electronic states in the ferromagnet and the inspection of the complex band structure of the insulating barrier.[49] For a quantitative ab initio estimation of P_i, one may turn in first approximation to the linear-response theory of tunneling as formulated within the Landauer theory of transport or, equivalently within the Kubo formula.[50] The computed tunneling conductances have a straigthforward interpretation in terms of the density of state of each transport channel duly weighted by a "transmission" coefficient associated with the overlap of the electron wave functions. Such a method has, for example, been used by the group of Kelly to predict the spin filtering properties at interfaces between Ni or Co ferromagnets and graphene or h-BN layers.[51–53] While the aforementioned approaches all consider the device at equilibrium, the bias dependence of the polarization is of great importance from the applications point of view. Over the last decade, the non-equilibrium Green's function formalism[54] has been used by a few groups to rationalize the spin-injection properties of various interfaces under finite bias voltage.[55–57]

In a lateral spin-valve device configuration as shown in Figure 2a, the spin information is first generated and injected by the spin polarizer. By applying a rather small bias voltage (typically in the 10 mV range), the spin information is then propagated within the channel carried by the electrical charge current.[58,59] Finally, it is detected by the spin analyzer[60] when absorbed within the ferromagnetic contact. The electrical resistance of the device is expected to vary depending on the relative configuration of the

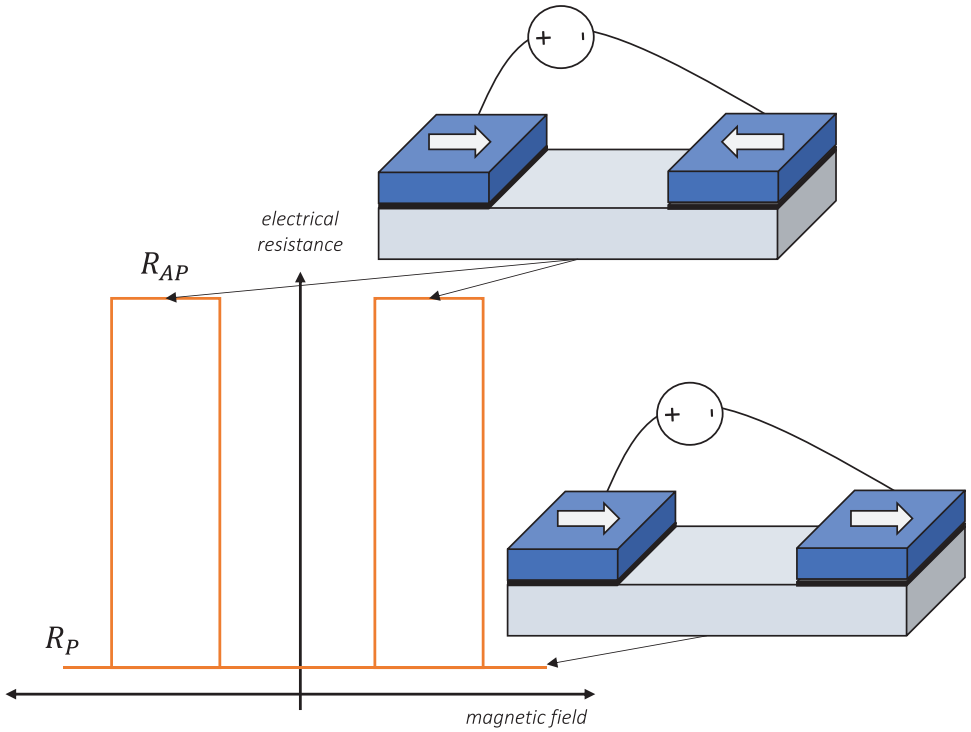

Figure 3. Magnetoresistive response of a spin-valve. The two configurations of the magnetizations (parallel and antiparallel) are represented. The two ferromagnetic electrodes must present different coercive fields in order to exhibit an antiparallel configuration. The spin signal ΔR is defined by the difference between R_{AP} and R_P.

magnetizations of the electrodes namely parallel (R_P) and antiparallel (R_{AP}) as illustrated in **Figure 3**. This change of electrical resistance with respect to an external magnetic field is caused by a magnetoresistance (MR) effect and is quantified by the following generic equation

$$\mathrm{MR}\,(\%) = \frac{R_{AP} - R_P}{R_P} \times 100 \tag{3}$$

The measured MR signal can be attributed to spin transport only if the spin information is conserved during the transport along the channel until it is detected by the second ferromagnetic contact. In other words, the spin lifetime (τ_{sf}) has to be larger than the dwell time within the channel (τ_n). Or the spin diffusion length (l_{sf}) characterizing the spin transport distance before losing the spin orientation has to be much larger than the distance (L) between the two ferromagnetic contacts.

In a standard model of spin transport in a two-terminals and confined geometry, the MR is described based on the original GMR formulations[21,61] by the following equation[62]

$$\mathrm{MR} = \frac{R_{AP} - R_P}{R_P} = \frac{P_1 P_2}{1 - P_1 P_2} \frac{2}{2\cosh\left(\frac{L}{l_{sf}}\right) + \left(\frac{R_b}{R^s_{ch}} + \frac{R^s_{ch}}{R_b}\right)\sinh\left(\frac{L}{l_{sf}}\right)} \tag{4}$$

R_b being the contact resistance between the channel and one the ferromagnetic electrode. The contact resistance can originate from the presence of a native Schottky barrier for instance or it can be intentionally tuned by intercalating a thin tunnel barrier for instance. R^s_{ch} is defined as the spin resistance of the channel material ($R^s_{ch} = \rho \times l_{sf}$) with ρ its electrical resistivity. We can already see with this spin transport model two different limits with respect to the R_b/R^s_{ch} ratio, illustrating the so-called "impedance mismatch" issue.[20] The corresponding derived equations for multiterminal devices are presented and fully discussed in the following references[14,62] but the following criteria remains also valid for multiterminal devices.[14]

If $R_b/R^s_{ch} \ll 1$: the spin relaxation occurs mostly within the spin polarizer due to spin absorption. The spin information has been lost even before reaching the first interface. The transported current within the channel is unpolarized as depicted in the **Figure 4**a (case (2)).

If $R_b/R^s_{ch} = 1$: it is the ideal condition for spin injection. However, the intrinsic spin lifetime or the spin diffusion length of graphene and carbon nanotubes is not known. It is thus difficult to estimate an intrinsic value for the spin resistance of graphene and carbon nanotubes as depicted in the Figure 4a (case (3)). It is particularly interesting to note that even in this specific case ($R_b = R^s_{ch} \gg R^s_F$ where R^s_F is the spin resistance of the ferromagnetic contact), the injected spin polarization is lower than the intrinsic spin polarization of the ferromagnetic contact itself.

If $R_b/R^s_{ch} \gg 1$: The spin relaxation occurs within the transport channel. The spin information is lost before being detected by the spin analyzer.

It is also intuitive to see that for a given channel with a given spin diffusion length, the MR signal should decay while

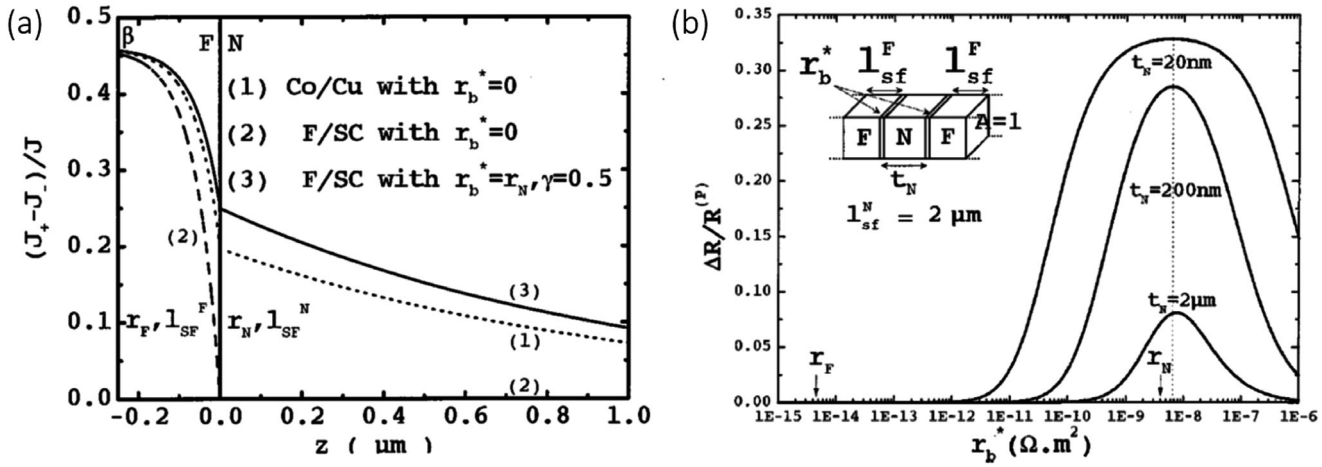

Figure 4. Illustration of the impedance mismatch issue. a) Calculation of the spatial profile of the injected spin polarization at (1) a Co/Cu interface, (2) a FM/SC interface without any contact resistance (noted here r_b^*), and (3) with an appropriate contact resistance. b) Calculation of the MR signal as a function of the contact resistance for different channel lengths (noted here t_N). γ is the spin polarization. Details of the calculations are given in the ref. [22]. Adapted with permission.[22]. Copyright 2001, American Physical Society.

increasing the channel length as calculated in Figure 4b. Effectively, the current slowly loses its spin polarization while propagating within the channel as represented in the Figure 4a for instance.

Concerning spurious effects in spin-valves, it is mandatory to ensure that the observed magnetoresistive effect originates from spin transport because there may co-exists other contributions from magnetoresistive effects not necessarily related to spin transport and that could perfectly mimic a spin-valve behavior like tunneling anisotropic magnetoresistive effects,[63] stray-field induced magnetoresistive effects linked to the intrinsic magnetoresistance of a carbon nanotube[64] or magneto-Coulomb effects.[65] Experimentally, there exists several options. It is possible to replace one of the ferromagnetic electrodes by a non-magnetic material like Cu or Au. In this case, the MR should totally disappear. Another method is to track the magnetoresistive response with respect to the angle between the magnetic field and the easy axis of the ferromagnetic electrodes. The magnetoresistance, if correlated to spin transport, should quickly disappear with respect to the angle between the polarizer and the analyzer. If correlated to tunneling anisotropic MR (TAMR[63]) for instance, the magnetoresistive response will survive and will even change its signs while respecting the symmetry of the device. Finally, an upgrade in the device's architecture with multiterminal geometries for non-local magnetoresistive measurements and Hanle effects is also mostly considered by the community.[66–72]

4. Spin Transport Experiments in Carbon Nanotubes

All experimental studies published so far and presented in this review are conducted by depositing the ferromagnetic metal directly in contact with a single carbon nanotube either single-wall or multiwall. This naïve approach is in striking contradiction with all the developments from the last 20 years concerning spin injection into semiconductors as discussed before.[20–22,62] Indeed, depending on the value of the R_b/R^s_{ch} ratio and the value of P, the spin information can either be inefficiently transmitted or even be lost before being detected.[14,22] This phenomenon dubbed "impedance mismatch"[20] was not really tamed by the community at the beginning of this activity in 1999 and therefore the devices were not necessarily optimized to maximize the spin injection and transport. Moreover, the intimate properties of metal/carbon nanotubes interfaces are still widely debated in the literature[73–77] but it is known that even a single material deposited as a contact over a carbon nanotube can display orders of magnitude of variation on the contact electrical resistance even on the same carbon nanotube.[78,79] All those factors bring a great disparity in the observations and in particular on the transport and injection regime and therefore on the interpretation itself of the magnetoresistance as presented in the following.

The first experimental report of spin transport in single carbon nanotubes date back to 1999 and come from Ago's group at the Cavendish Lab in Cambridge, UK.[80] It concerns devices in which multiwall carbon nanotubes deposited on a Si/SiO_x substrate are contacted directly by two ferromagnetic electrodes of Co ($P_{Co} \cong 35\%$)[81] separated by a distance of the order of 250 nm taking up the concept of spin-valves. An image of the device investigated in this study is illustrated in **Figure 5**a. Magnetoresistance effects of the order of +1% to 2% at 4.2 K (as shown in Figure 5b) are reported to rapidly decrease and disappear for temperatures of the order of 25 K. The resistance of the devices varies from 10 to 250 kΩ as shown in Figure 5b. A quasi-ballistic charge transport in the multiwall carbon nanotube is envisaged by the authors in a later publication in 2001.[82]

A second study published in 2002 by Schneider's group at IFW Dresden in Germany shows in Co/multiwall carbon nanotube/Co device with a separation between the contacts of the order of 200 nm, an example of which is shown in Figure 5c, much greater MR effects up to + 30% at 4.2 K and for a low current of 1 nA.[83] An example of 15% magnetoresistance is shown in Figure 5d. In these devices, the electrical resistance is greater than those of Ago's group (10–100 kΩ) and reaches 2.4 MΩ at 4.2 K. It is mainly attributed to the contact resistance between

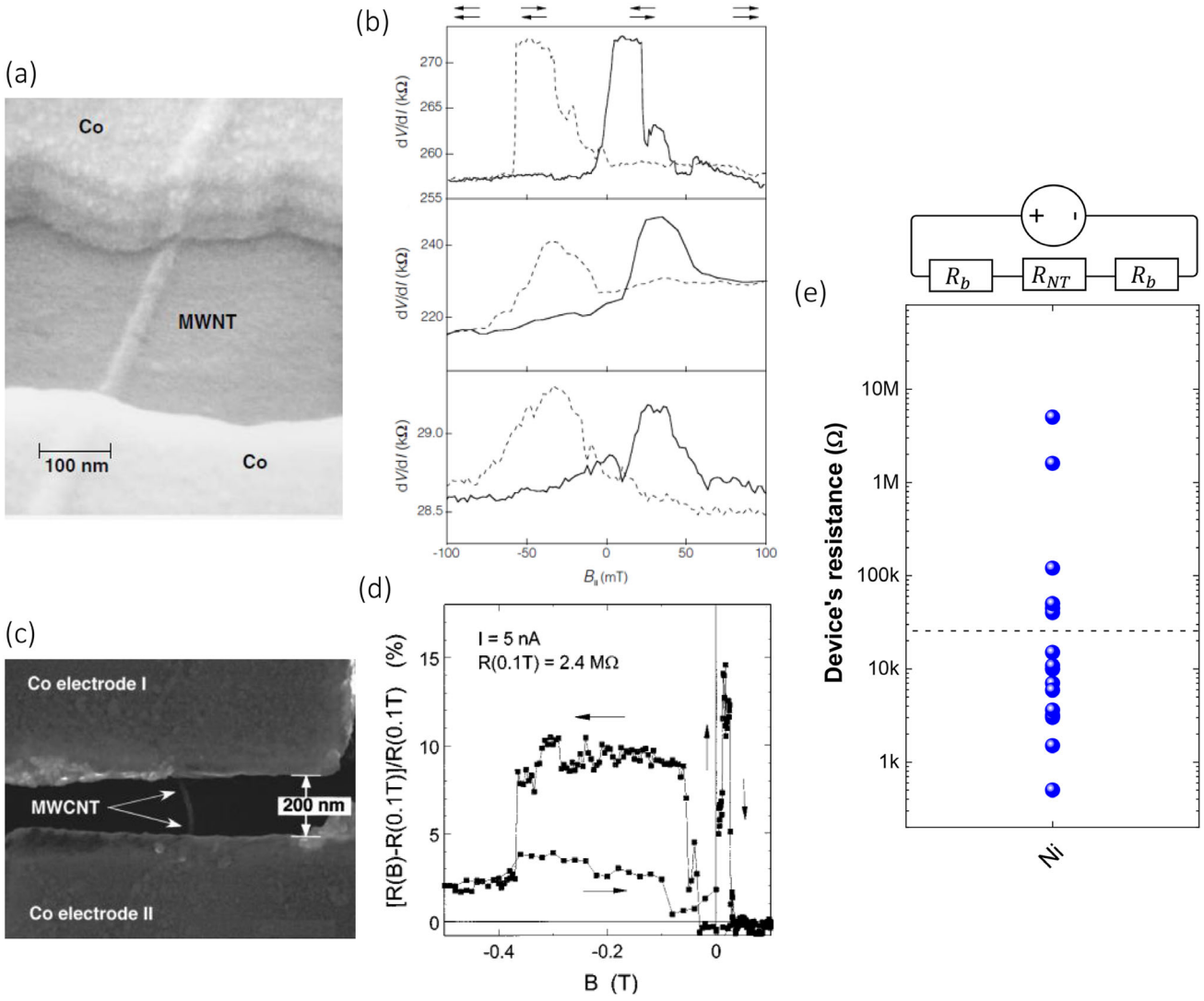

Figure 5. Magnetoresistance in carbon nanotubes-based spin-valves. a) Scanning electron microscope image of two Co contacts separated by a multiwall carbon nanotube. The gap distance is 250 nm. b) Magnetoresistive signals ranging from 1% to 2% of different devices measured at 4.2 K. a,b) Adapted with permission.[80] Copyright 1999, Springer Nature. c) Scanning electron microscope image of two Co contacts separated by a multiwall carbon nanotube. The gap distance is 200 nm. d) Magnetoresistive signal of 15% measured at 4.2 K. c,d) Adapted with permission.[83] Copyright 2002, AIP Publishing. e) Variation of device resistance for multiwall carbon nanotubes contacted with Ni. The equivalent circuit of the device is shown above. Adapted with permission.[79] Copyright 2016, AIP Publishing.

the Co and the multiwall carbon nanotube whose resistance is rather around the kΩ range.[84] In this study, the transport in the carbon nanotube is also assumed to be quasi-ballistic. Magnetoresistance effects also decrease rapidly with the current applied through the carbon nanotube reaching a near-zero MR signal around 50 nA. A third study in 2002 by Kim's group concerns Co/single wall carbon nanotube/Co with separations between the electrodes of Co varying between 420 nm and 1.5 µm. MR effects between +2.6% and +3.2% are reported at 100 mK for channel lengths of 1.5 µm and 450 nm respectively. These devices present fairly large resistances greater than 10 MΩ showing, according to the authors, a transition to the Coulomb blockade transport regime.[85]

Those first studies were followed by a large collection of articles[86–92] all investigating spin transport in the Coulomb blockade regime.[93,94] Most of those references are discussed in the following review proposed by Cottet et al.[95] We will not again review in detail those articles because the phenomenology in the transport step is very different and does not consider parameters like the spin diffusion length. However, an important subconclusion can be formulated based on those studies: the ferromagnetic contacts were directly deposited above the carbon nanotube giving a wide range of device's electrical resistances and showing no clear control of the electrical properties.[78,96] As a striking example, the study by Preusch et al., reveals that $Pd_{60}Fe_{40}$ contacts evaporated on the same nanotube can present variations in the contact resistance (R_b) between 20 kΩ to 1 MΩ.[78] Figure 5e also reveals this variation in the case of the multiwall carbon nanotubes contacted with Ni electrodes ($R_{dev.} = 2R_b + R_{NT}$ while R_{NT} is of the order of few kΩ[29]).

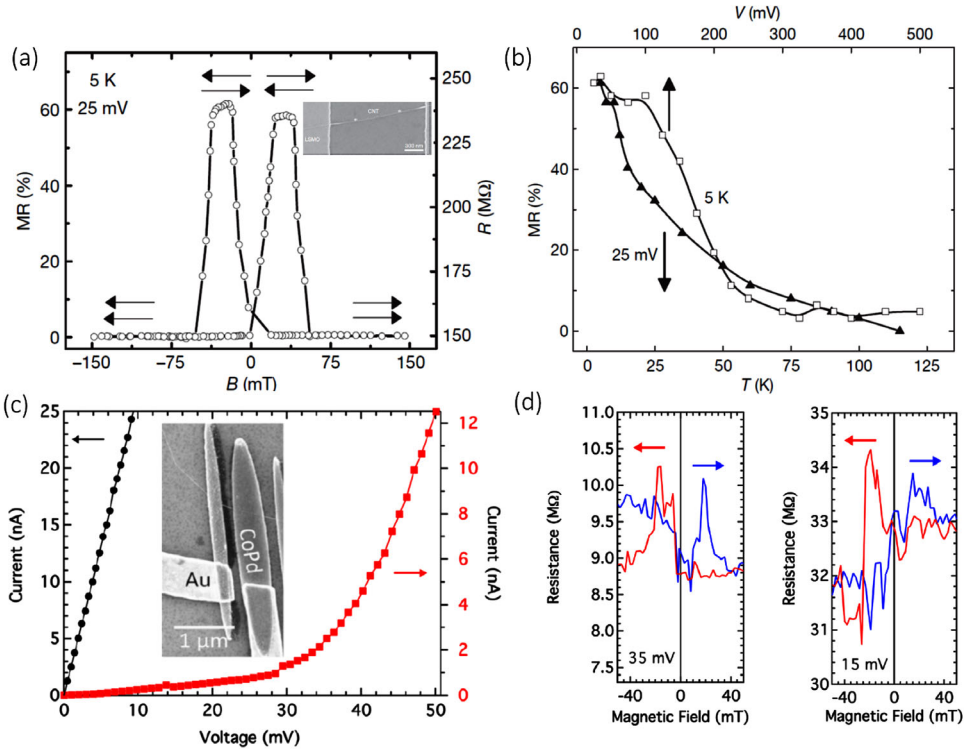

Figure 6. Recent spin transport studies in carbon nanotubes. a) Magnetoresistive signal of +60% measured at 5 K and V = 25 mV in a LSMO/mutliwall carbon nanotube/LSMO device. An electron microscope image of the device is shown in inset. b) Magnetoresistive signal versus temperature (empty square) and bias voltage (filled triangle). a,b) Adapted with permission.[98] Copyright 2007, Springer Nature. c) Current–voltage characteristics of CoPd/carbon nanotube/CoPd measured at 300 K (black dots) and 4 K (red squares). d) Magnetoresistive signals measured in different devices at 4 K and 35 mV (left) and 15 mV (right). c,d) Adapted with permission.[101] Copyright 2016, American Physical Society.

To summarize, until 2007, spin lifetimes for charge carriers in a carbon nanotube reported experimentally in the literature have been estimated between 3 ps and 3–5 ns.[95] Theoretically, there is practically almost no calculation giving the intrinsic spin lifetime in a carbon nanotube. Lafrate's group at North Carolina State University has, as the only example, estimated the spin lifetime to 1 s.[97] Regarding the spin diffusion length, it is, until this date, limited to 1.5 μm which corresponds to the inter-contact distance of the devices from the Kim's group reported during the first experiments of 2002.[85] As we will show now, these values were largely improved by playing with R_b and P.

In 2007, Mathur's group in Cambridge in collaboration with Fert and Littlewood published a major article in Nature[98] reporting significant magnetoresistance effects of the order of +60% in La,Sr(MnO_3)/multiwall carbon nanotube/La,Sr(MnO_3) ($P_{LSMO} \cong 90\%$)[99] devices with inter-electrode distances of the order of 1.5 μm and an electrical resistance of 150 MΩ (i.e., $R_b \cong 75$ M $\gg R_{NT}$). An example of a +60% magnetoresistance effect is shown in **Figure 6**a with an image of the device in inset. Figure 6b illustrates the voltage and temperature dependence of the magnetoresistive signal which disappears for voltages of 450 mV and temperatures around 75 K well below the Curie temperature of the LSMO being around 300 K.[100] With the following spin transport derived from the main formula presented before

$$\mathrm{MR} = \frac{R_{AP} - R_P}{R_P} = \frac{P^2/(1-P^2)}{1 + \tau_n/\tau_{sf}} \quad (5)$$

the authors were able to estimate, at a minimum, spin diffusion lengths of 50 μm and relaxation times of the order of 30 ns.

These large spin diffusion lengths were reported experimentally for the first time in a non-magnetic material.

Following this publication, there have been some very interesting studies all from the Meyer's group in Jülich.[101–103] In particular, this team focused on the impact of the native tunnel barrier between CoPd contacts ($P_{CoPd} \cong 25\%$)[101,102] and a (single and multiwall) carbon nanotube on the amplitude of the MR effects. They showed that the MR increases when the contacts are resistive (>100 kΩ) especially at low temperatures compared to simple ohmic contacts whose resistance does not vary much with temperature. Current–voltage characteristics at 300 K (in black) and 4 K (in red) are, for example, presented in Figure 6c for a CoPd/carbon nanotube/CoPd device with resistive contacts revealing a clear decrease in the current level at 4 K. Two examples of MR curves with contact resistances varying between 4 and 15 MΩ are also illustrated in Figure 6d. Thanks to Hanle measurements in more complex non-local geometries,[104] this group also reported spin lifetimes of the order of $\tau_{sf} = 1.1$ ns even if this technique is known to underestimate the effective spin lifetime.[105] Spin transport effects in non-local geometries had also been presented and discussed as early as 2010 by the Kontos' group without however providing quantitative information about the spin lifetime.[106]

In this section dedicated to spin transport in carbon nanotubes, we are able to highlight several aspects of this topic:

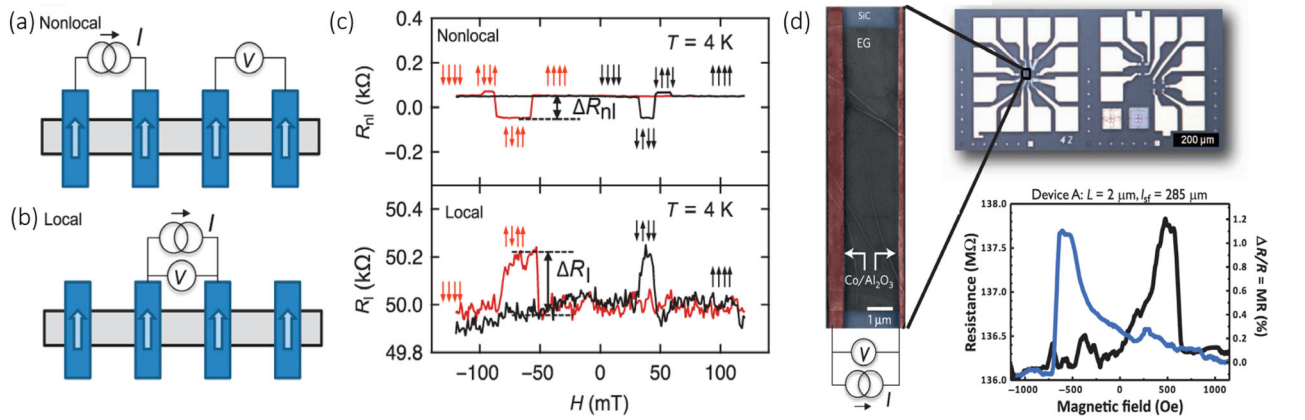

Figure 7. Lateral spin transport in graphene channels. Two main configurations are analyzed in the literature. a) The non-local measurements are based on the injection of the current in on set of electrodes and the measurements of the spin induced potential variations in a second set of electrodes. The decoupling of charge and spin transport allows to reach less noisy spin signals thus more easily observed if small. b) The local configuration use only one set of electrodes mixing charge and spin transport as in usual GMR and TMR-based devices. c) Early results starting in 2006 have pinpointed sizeable spin signals in both local and non-local configurations, highlighting the strong potential of graphene for spin transport. d) Introduction of highly confined graphene channels (high impedance tunnel contacts, confined two-contact geometries, shielded transport) leads overall to larger spin signals. a,b) Adapted with permission.[14] Copyright 2012, Springer Nature. c) Adapted with permission.[122] Copyright 2012, Elsevier. d) Adapted with permission.[123] Copyright 2012, Springer Nature.

1) The low representation of spin transport studies in quasi-ballistic and/or diffusive regimes where there is finally only one major result published in 2007 showing $l_{sf} > 50\ \mu$m and $\tau_{sf} > 30$ ns.
2) The rather limited use of highly spin-polarized contacts (only one study[98]).
3) The lack of characterization and control of barriers at ferromagnetic metal/carbon nanotube interfaces leading to disparate injection properties: 120 MΩ > R_b > 5 kΩ.

Those two last points are also valid for studies related to spin transport in graphene, as presented in the next section.

5. Spin Transport in Graphene

Starting in 2004–2005, graphene has been made available for device integration following the seminal work of Geim et al. based on exfoliation.[107] Exceptional spin transport expectations for graphene have been formulated early, with predicted spin diffusion lengths above the 100 μm range for this crystalline material.[40] Similarly to works on metals,[108] semiconductors,[109–111] and carbon nanotubes,[98] lateral spin valve geometries based on graphene have been then studied (both in local and non-local multiterminal configurations, see **Figure 7**a,b), in an attempt to extract graphene intrinsic spin transport properties. As early as 2006, initial experiments with pioneering lateral spin valves based on exfoliated graphene flakes connected to NiFe electrodes have been presented,[112] with unspecified contact interface nature and resistance. This has been followed by works of different teams in the 2007–2010 period including seminal studies by Ohishi et al.,[112] Tombros et al.,[68] Cho et al.,[112] Goto et al.,[112] Popinciuc et al.,[113] and Han et al..[114] These pioneer works revealed exciting results of successful spin transport in different graphene channel configurations, with sizeable spin signals for channels extending over several microns (see Figure 7c). Most of these early works on graphene reveal spin lifetimes of about 1 ns and spin diffusion lengths below few μm. It thus appeared that the measured properties are well below theoretical expectations for graphene and early experimental results on carbon nanotubes.

This raised the question of the physical origins of the quenching of the extracted graphene spin properties: device's architecture and environment (interaction with the substrate or atmosphere), purity of the materials, control of the interfaces, and more specifically the precise role of contacts in the depolarization of spin currents. This last point has been already a strong drag for the study of conventional semiconductors as spin channels.[22] Reported variations between the cited seminal studies can already be, even partially, attributed to contact definition protocols. When available, oxide barriers descriptions depict mostly inhomogeneous properties[113] typically of evaporated ultrathin films on graphene, and resistance-area products are set in the 1 to few 10 kΩ μm^2. Following this early set of studies of graphene spin transport properties (see more details in review in ref. [115]), progressive optimization of the devices with for instance the integration of h-BN layers as a way to isolate the graphene layer from the substrate and the environment, or also using h-BN also as a tunnel barrier, led to remarkable increased spin properties for exfoliated graphene, with spin relaxation lengths reaching the 10–100 μm range.[66,69,116–118]

This large dispersion of values over several orders of magnitude for the spin relaxation lengths tends to indicate that the measured properties were finally not fully and intrinsically related to graphene, but were also influenced by different device's parameters and configurations. As an example of this debate, Idzuchi et al., have investigated the underestimation of the spin lifetime in graphene-based devices due to spin absorption induced by invasive ferromagnetic electrodes.[105] As for carbon nanotubes or every inorganic semiconductor, the role of the contact interfaces with the spin sources is well understood to be critical for the preservation of the spin lifetime in the overall device. As previously discussed, the $R_b/R^s_{ch} = 1$ criteria remains a

primordial condition to fulfill being in a 2-terminal or 4-terminal geometry.[14,21] It has also been discussed that transport properties in a device with tunnel contacts but with extended channel and multiple contacts can be detrimental to the spin signal.[62,119] Illustratively, a leaky contact deposited on the channel, even if located further away from the probed area, can act as a strong spin-sink for the device properties,[120] while this situation has been neither discussed or even less systematically analyzed in the literature. This lets open clear perspectives for further enhancement of graphene spin transport properties exploitation.[119,121]

In this direction, focusing on multilayer graphene grown epitaxially on SiC, Dlubak et al.[123] have investigated spin transport in a highly confined device configuration, where multilayer graphene shields the inner transport channels which are further strictly limited to the space between the two spin-polarized tunnel electrodes (see Figure 4d). This has been deemed the optimal configuration to reach the intrinsic properties of the channel.[62] Furthermore, sputtered high quality Al_2O_3 tunnel barriers have been used to prevent the impedance mismatch situation of leaky contacts and reach the high impedance regime described in seminal spin transport formalism[22,61] (right side of the bell-shaped curve of Figure 4b). Indeed, reported resistance-area products for the contacts developed in this study achieve values of 1 MΩ μm^2 and higher, setting the devices in the high contact resistance transport regime with extended spin dwell times. A non-leaky tunnel barrier prevents also the hybridization effects of graphene with the ferromagnetic metals, a possible source of spin information loss during spin currents transport in non-ideal devices.[124] In the specific confined configuration of ref. [123] graphene spin lifetimes have been measured in the 100 ns and spin diffusion length well above 100 μm, in-line with the increase of spin properties expected while reaching a fully confined scenario (closing on the intrinsic graphene capabilities). While this result is much more in-line with early carbon nanotubes measurements[98] and initial theoretical expectations,[40] this might still represent only an underestimate of graphene potential.

Overall, these different works based on graphene have undoubtedly highlighted the crucial role of interfacial contacts engineering for efficient spin injection. Most of these works focus on usual inorganic insulators, either well demonstrated tunnel barriers Al_2O_3 or MgO, or other insulators such as TiO_2, with different deposition techniques leading to varied results for a given material.[113,115,125] More recently 2D h-BN has also been introduced as a tunnel barrier for spin devices.[126,127] The main discussed objective for the use of a tunnel barrier in graphene based devices has been so far on reaching a passive resistive interface to prevent spin back-flow and losses.[14,22] Interestingly, we note that h-BN already offers the possibility to tailor its spin properties by proximity effects and hybridizations thanks to its 2D nature with reported strongly increased spin polarizations,[128] as such it represents the first step toward more control over interfacial spin transport.

6. Interest for Developing New Barrier Materials for Spintronics in Carbon-Based Materials

As discussed before, the insertion of a well-calibrated tunnel barrier between the ferromagnetic contact and the graphene channel in graphene-based spin-valves has been a key technological element to drastically promote spin signals (defined as $\Delta R = R_{AP} - R_P$) from 10^3 to 10^6 Ω and thus the spin diffusion length from 1 μm up to 200 μm during the past few years.[14,123] As discussed previously, the properties of the injection barrier dictate the MR response of a lateral device thanks to two physical parameters: the interfacial spin polarization (P) from the spin polarizer and detector and the interfacial electrical resistance (R_b).

In graphene, the pioneering work of Tombros et al. was conducted using a 0.6 nm thick Al oxide layer on graphene deposited thanks to evaporation under high vacuum conditions.[68] On the other hand, Dlubak et al. characterized sputtered Al_2O_3 and MgO ultrathin layers deposited on graphene.[125] Sputtering is an industrial deposition method to grow high quality ultrathin tunnel barriers especially for spintronics devices such as magnetic tunnel junctions.[129] However, all those physical deposition techniques are not necessarily compatible with carbon nanotubes due to their peculiar shape. Being quite anisotropic, those deposition methods can induce shadow effects and lead to uncovered parts of the carbon nanotube with the tunnel barrier. For instance, if a carbon nanotube is deposited over a flat substrate, this type of anisotropic deposition method will cover only the upper part of the nanotube and will let the side and its part in contact with the substrate completely uncovered leading for instance to spatial variation of doping. It is thus mandatory to use more isotropic methods. One recent technique with such properties is named atomic layer deposition (ALD).[129] In 2014, Martin et al. have successfully implemented this technique to grow thin Al_2O_3 tunnel barriers over graphene with similar properties than with the standard sputtering method but with the benefit of a conformal layer by layer growth.[124,130] This ALD approach has also been extended later to MgO tunnel barriers.[131,132] There exist few attempts in the literature using ALD to grow ultrathin barriers over carbon nanotubes but not yet for spintronics applications.[133,134] One alternative promising path lies in surface chemistry. Carbon surfaces such as graphene and the outer shell of a MWNT are perfect platforms for chemistry especially for using C—C chemical bonds.[135–137]

7. Advantages of Hybrid Molecular Barriers

7.1. Engineering at the Atomic Scale of the Spin Polarization

Molecules at the interface with a metal are known to chemically hybridize with the metallic surface.[138,139] The quantum interaction at the interface can strongly impact the electronic structure of the molecules but also of the metal.[140] This hybridization has also been described more recently in the specific case of ferromagnetic metallic surfaces.[141–144] It was originally proposed for explaining apparently divergent observations in magnetotransport experiments in (La,Sr)MnO_3/Alq_3/Co organic spin-valves.[141,145,146]

Indeed, the discrete orbitals of the molecule tend to be affected by the quantum coupling with the spin states of the nearby ferromagnetic metal as depicted in the **Figure 8**a. The chemical reaction of the molecule with the metal can give rise to a chemical bond in the case of strong coupling (like for the first Alq_3 layer over Co as shown in Figure 8b) or to a weaker interaction similar to van der Waals interactions in case of physisorption for instance.[139] As a result of this quantum interaction and

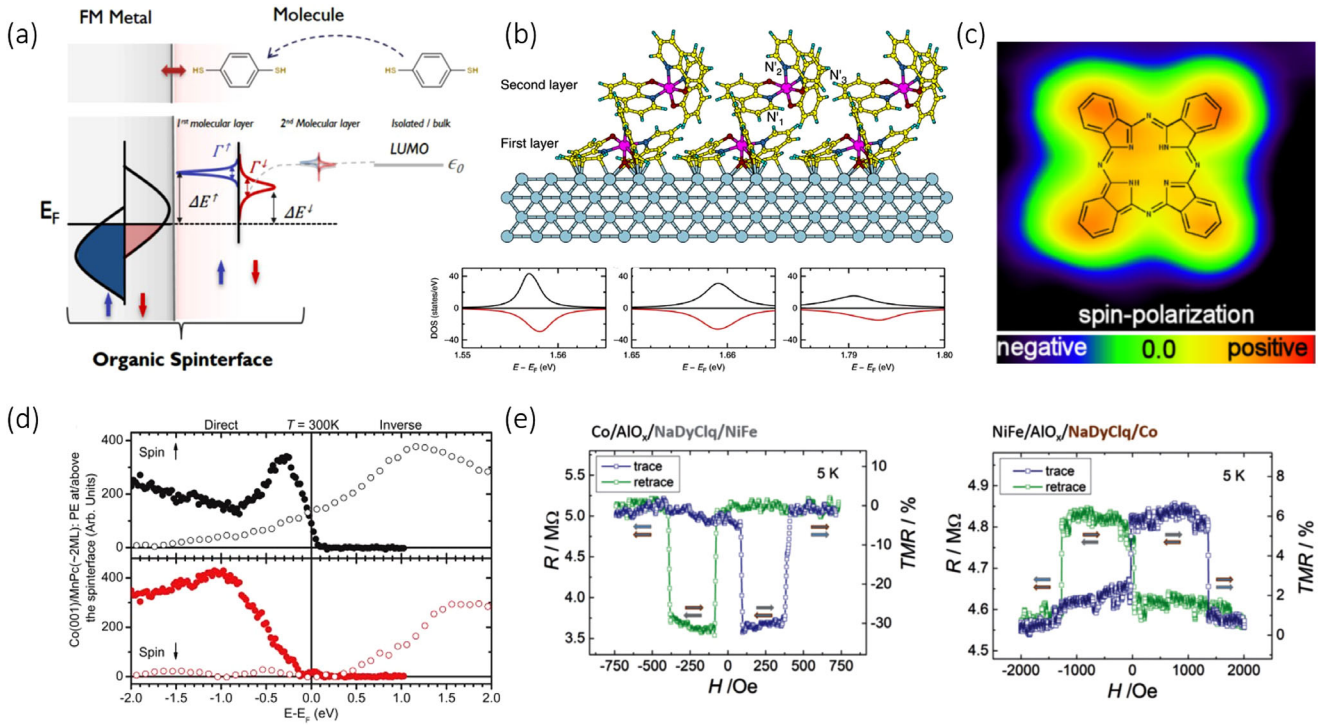

Figure 8. a) Hybridization of a discrete molecular orbital (here the lowest unoccupied molecular orbital) with a ferromagnetic surface. The orbital tends to be shifted ($\Delta E^{\uparrow\downarrow}$ terms) in energy and broadened ($\Gamma^{\uparrow\downarrow}$ terms) in a spin dependent way. Adapted with permission.[147] Copyright 2018, IOP Publishing. b) Chemical structure of two layers of Alq_3 molecules deposited over a Co surface. Three calculations corresponding to the three N (N'_1 (left panel), N'_2 (middle panel) and N'_3 (right panel)) atoms from an Alq_3 molecule belonging to the top layer revealing the shift and broadening of a molecular orbital are shown below. Adapted with permission.[148] Copyright 2016, Springer Nature. c) Reversal of the spin polarization observed at a H_2Pc/Fe interface thanks to spin polarized scanning tunneling spectroscopy. d) Spin polarized photoemitted current with respect to the energy for both spin directions measured at a Co/MnPc interface. Only the signal from the majority spin direction crosses the Fermi energy meaning that this interface is highly spin polarized ($P \cong 100$ %). Adapted with permission.[149] Copyright 2016, American Chemical Society. e) Reversal of the sign of the magnetoresistive signal thanks in organic spin valve due to the change in sign of the top interface spin polarization ($P_{NiFe/NaDyClq} < 0$ and $P_{Co/NaDyClq} > 0$). Adapted with permission.[150] Copyright 2018, Wiley-VCH GmbH.

depending on its strength, the discrete molecular orbitals are broadened (Γ) in energy and can also be shifted in energy (ΔE)[138,151,152] sometimes becoming even metallic. The spin dependent nature of the electronic density of states of the magnetic surface imposes that the shift and the broadening become also spin dependent ($\uparrow\downarrow$).[13,153,154] As a consequence of the presence of those interfacial hybridized states, the ferromagnetic metal/molecule interface can be described for magnetotransport as an effective magnetic electrode acting as a spin source comprising the hybridized molecular interfacial state in addition to the metallic states.[141,147] This hybrid electrode is named "organic spinterface" on Figure 8a. Effectively, in magnetotransport experiments, it is this last hybridized state which dominates and imposes the value and the sign of the spin polarization of the emerging current into the organic film and of the spin detector. The almost infinite variety of organic compounds available have paved the way to an on-demand atom by atom engineering of spintronic properties of hybrid interfaces.[13,153,154] As a flagship, molecules such as phthalocyanines have demonstrated that changing only the central atom could provide a sufficient lever to completely tune the interfacial spin polarization.[155–160] It has also been reported that for a given molecule, a change in the ferromagnetic metal can lead to a drastic change in the coupling and thus on the sign of the emerging spin polarization for instance (see Figure 8e for the case of the NaDyClq molecule for instance).[150,161]

In terms of tailoring of the spin polarization, two main cases of interest were deduced from calculations and/or experiments (spectroscopy, magnetotransport, and so on):

1) A reversal of the sign of the initial spin polarization (**Figure 9**a). The hybridized states of the molecule present an effective spin polarization with an opposite sign than that on the ferromagnetic surface alone (it may also modify the amplitude of the spin polarization). It corresponds to the iconic cases of the $(La,Sr)MnO_3/Alq_3$[141] and Fe/H_2Pc[162] interfaces shown in Figure 8c.

$$P_{FM} = -P_{FM/mol} \tag{6}$$

2) An enhancement of the initial spin polarization often referred as spin filtering (Figure 9b). The hybridized molecular states reinforce by an additional spin filtering mechanism the spin polarization of the current emerging from the ferromagnetic surface. Such cases were reported for instance at the Co/Alq_3 interface,[141,148,163] Co/MnPc interface (shown in

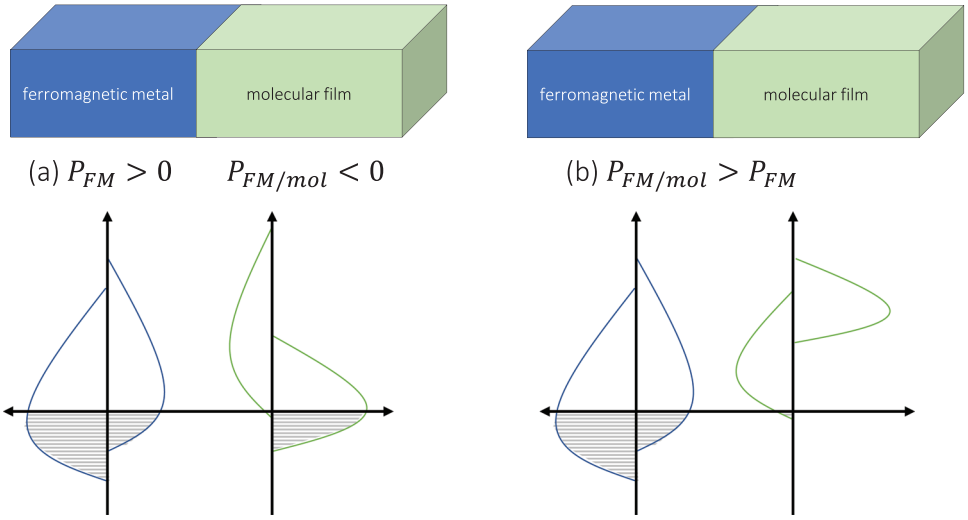

Figure 9. a) Case of the reversal of the initial spin polarization emerging from the ferromagnetic surface. b) Case of the enhancement of the emerging spin polarization.

Figure 8d)[149] and to the Co/ZMP interface[164] but also widely in other systems,[157,165–172]

$$P_{\mathrm{FM}} < P_{\mathrm{FM/mol}} \tag{7}$$

In this last case, it is common to express this enhancement in terms of spin filtering efficiency (SFE) as $\mathrm{SFE} = P_{\mathrm{FM}}/\mathrm{mol}/P_{\mathrm{FM}} \times 100$[173] which could reach values as high as 85% in the case of Co/CuPc interfaces.[173]

7.2. The Perfect Match in Terms of Chemistry

The chemical functionalization of graphene and carbon nanotubes is a vast topic of research. Several reviews have been written on this pluridisciplinary field.[174–179] It offers powerful levers in order to tune the electronic,[180] mechanical,[181] or optical[182] properties of the carbon-based nanomaterials. Technologically, it is possible to distinguish between two main chemical approaches for the functionalization which depend on the strength of the interaction between the molecule and the graphene or the carbon nanotube surface:

1) The physisorbed approach (weak interaction),
2) The chemisorbed approach (strong interaction).

The physisorbed scenario includes interactions like π–π interactions, van der Waals interactions, H bonding or ionic interactions.[183] In all those cases, the π-conjugation related to the sp^2 hybridization of the C atoms forming the graphene or the carbon nanotube is conserved even after the functionalization. The adatoms or the adjacent molecules will slightly perturbate the electronic structure of graphene or of the carbon nanotube and might also lead to charge transfer[184–189] and thus doping. In this sense for instance, carbon nanotubes and graphene are excellent and extremely precise gas sensors.[190–192]

In the chemisorbed scenario, there exists several alternatives with radicals, carbene, nitrene, or aryne species[193] described in Figure 10. Each of those approaches will lead to different chemical bonding with the graphene or with carbon nanotubes. The diazonium approach will lead to a single covalent C—C bond between the molecule and the C surface.[194–196] Carbene moieties will attach with two C atoms from the surface[181] like aryne[181]. A single nitrene molecule will produce N—C bonds with a single N atom attached to two different C atoms from the surface[183]. In all those cases, the C atoms from the graphene surface or from the outer shell of the carbon nanotube will rehybridize from a conducting sp^2 configuration into an insulating sp^3 configuration.

8. The Winning Combination

As discussed before, there are obvious technological and fundamental interests in combining carbon nanomaterials such as graphene and carbon nanotubes with organic molecules:

1) Very strong spin polarizations (P) can be reached with an on-demand atom-by-atom tunability of the interfacial spintronic and electronic properties;[149,197]
2) A perfect compatibility in terms of chemistry with extremely stable configurations such as the covalent coverage of carbon nanotubes with diazonium-based molecules for instance;[79,198,199]
3) A stability also with respect to standard CMOS technological fabrication processes.[200–202]

A recent study from Vera–Marun's group in Manchester shows an increase in the spin injection efficiency (namely the spin polarization) by a factor of two, thanks to the covalent functionalization of graphene compared to devices without any chemical functionalization.[203] The group reported on the use of benzoyl peroxide molecules grafted over graphene thanks to irradiation. Surface characterization reveals a decrease of the rms roughness of the Al_2O_3 grown after chemical functionalization from 1 nm to less than 0.5 nm. The high quality of the Al_2O_3 injection barrier and thus of the interface with the ferromagnetic metal (Co) leads

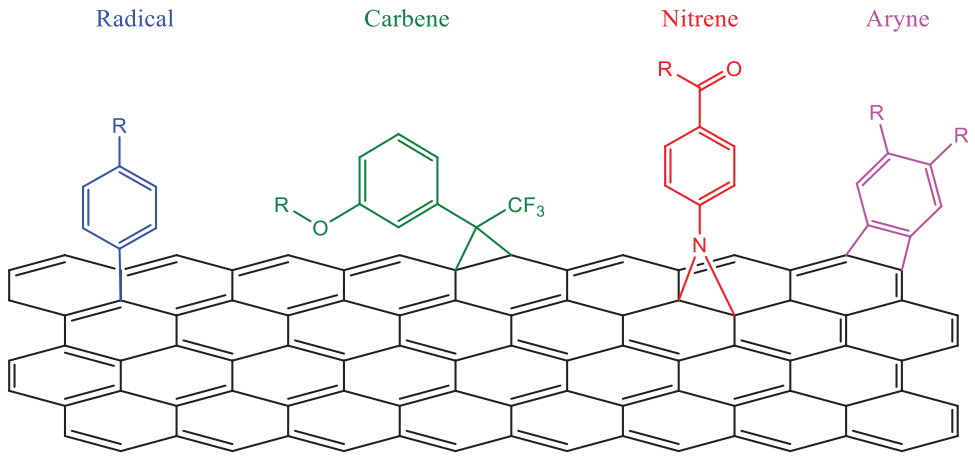

Figure 10. Graphene chemical functionalization via radical, carbene, nitrene, or aryne cycloaddition.

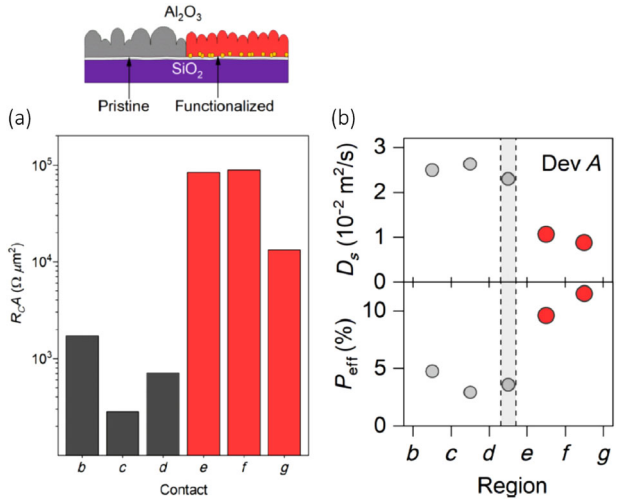

Figure 11. a) Resistance-area product for the Co/Al_2O_3 contact grown over graphene. The grey bars represent the contacts without any functionalization. The red bars represent the contacts with functionalization. b) Comparison of the spin diffusion coefficient and contact spin polarization between regions without (gray points) and with functionalization (red points). Adapted with permission.[203] Copyright 2021, American Physical Society.

to a increase by almost two orders of magnitude of the resistance-area ($R_b \times A$) product of the contact (from $10^3 \Omega\,\mu m^2$ to $10^5 \Omega\,\mu m^2$) as shown in **Figure 11**a and by a factor two in terms of spin polarization from $P = 4\%$ to $P = 10\%$ as shown in Figure 11b. The effect of the interface roughness with the spin polarization was already well detailed in the literature about magnetic tunnel junctions.[204–206] Other works have introduced functionalized or molecular graphene interfaces as well[203,207,208] with a strong potential for tailoring, but focusing so far only on their use as a seed or substitute for more difficult to control inorganic tunnel interfaces. Those efforts did not take full advantages of ferromagnetic metal/molecules interfaces.

In 2020, the observation of giant spin signals in functionalized MWCNT using nitro-benzene diazonium (NB) molecules covalently attached to the outermost shell of the MWCNT were reported.[79] The idea of the covalent functionalization of the outershell of a multiwall carbon nanotube was to positively combine different effects such as the strong spin polarization offered by the molecule/ferromagnetic metal interface and to redirect the electron and spin flows through the inner conducting shells of large diameter ($d > 60$ nm) multiwall carbon nanotubes intrinsically more protected from the environment. The redirection of the current through the inner shells was already demonstrated by the group of Martel in the case of functionalized double-wall carbon nanotubes (DWNTs).[209,210] The results are depicted in **Figure 12**. As expected the functionalization of a SWNT reveals a dramatic decrease of the current in the transistor configuration, whereas the current of functionalized DWNT is comparable to the non-functionalized SWNT one (Figure 12b). In Figure 12c three different signatures have been observed in DWCNT devices corresponding to the theoretical distribution of electrical behavior for DWNTs. Moreover, the reversible process (functionalization/annealing) is an efficient way to identify the electrical combination of walls forming the DWNT. In case of MWCNT, the presence of the molecules at the surface is also creating an injection barrier of $R_b = 1 - 100\ M\Omega$ whereas the pristine NT has a larger distribution of injection barrier as illustrated in **Figure 13**a. A high-resolution transmission electron microscope image of a functionalized MWCNT is also displayed in Figure 13b and allows determining the thickness of organic layer.

Density functional theory calculation revealed strong spin polarization of the Ni/NO_2 group interface of the order of +60% as shown in Figure 13c with the red line, thus predicting very efficient spin transport through the MWCNT with record spin diffusion lengths of the order of the millimeter and spin lifetimes of the order of 800 ns.[211] Such an efficient spin transport was also confirmed experimentally with the observation of magnetoresistive signals at low temperatures. In the Figure 13d, a signal close to −40% was measured very close to the theoretical limit of −50% as imposed in Equation (1). These examples demonstrate the particular interest of using organic thin film in spintronic carbon-based devices. These studies also suggest that the control of the metal/molecule interface is a key issue to enhance spin injection/detection into carbon-based devices.

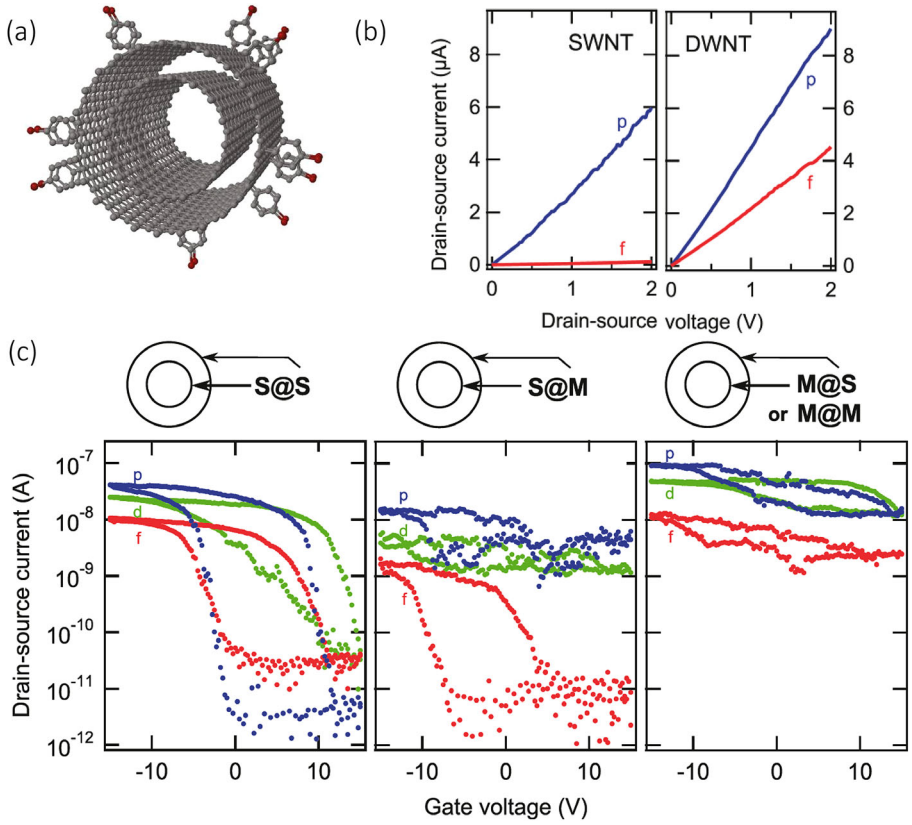

Figure 12. a) Schematics of a double-wall carbon nanotube (DWNT) for which the outershell is selectively functionalized by 4-bromo-phenyl molecules based on a diazonium reduction process. b) Current through carbon nanotubes with (red line) and without (blue line) functionalization for SWNTs (left) and DWNTs. After chemical functionalization, a SWNT becomes insulating. c) Gate spectroscopy of four types of DWNT after functionalization (S = semiconducting, M = metallic). Only the innershell conducts the current (blue points: pristine DWNT, red points: functionalized DWNT, green points: defunctionalized DWNT). Adapted with permission.[209] Copyright 2011, American Chemical Society.

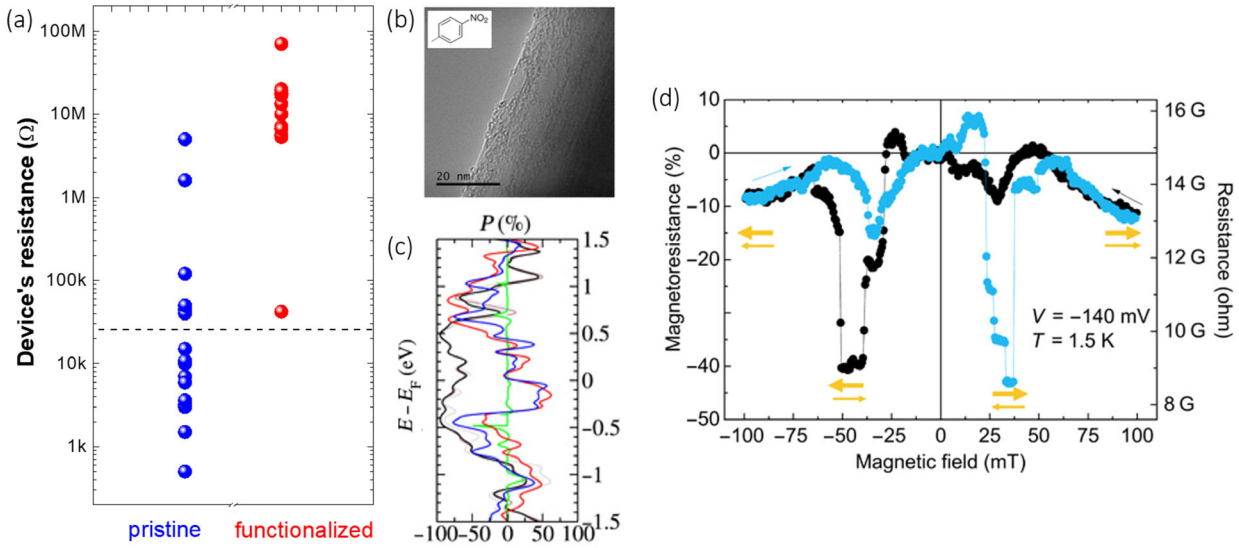

Figure 13. a) Effect of the covalent functionalization of NB molecules on the device's resistance. The increase of the device's resistance in the case of functionalized carbon nanotubes (in red) originates from the contact resistance (R_b). Adapted with permission.[79] Copyright 2016, AIP Publishing. b) High resolution transmission electron microscope image of a NB-functionalized multiwall carbon nanotube. The molecule is shown in the inset. c) Calculated spin polarization of the Ni/NB molecule/MWCNT interface (green line: outershell of the MWCNT, blue line: benzene ring, red line: NO_2 group, black line: surface Ni layer). d) Magnetoresistive signal measured in a device with a functionalized multiwall carbon nanotube showing a −40% effect while the theoretical limit is −50%. b–d) Adapted with permission.[211] Copyright 2020, American Association for the Advancement of Science.

9. Conclusion

Carbon-based nanomaterials such as carbon nanotubes, graphene, and molecules represent a class of physically complementary and chemically compatible materials. More specifically to spintronics, they offer different advantages such as high electronic mobilities, weak spin scattering, hybridization leading to strong spin polarizations fulfilling the core requirements of spintronic devices. In this perspective, first technological attempt to combine those nanomaterials for spintronics already reveal excellent characteristics such as outstanding spin diffusion lengths. We focus on the physical and chemical compatibility between the materials to reach exceptional figures of merit in the next generation of spintronics devices. As reviewed in the present article, this innovative approach requires strong developments in surface chemistry, spin transport physics, and theoretical descriptions of devices.

Acknowledgements

This project received funding from the F.R.S.- FNRS of Belgium, from the European Union's H2020 Future and Emerging Technologies Graphene Flagship (Grant Core3 No. 881603), from the Flag-ERA JTC 2019 project entitled "SOGraphMEM" (ANR-19-GRFI-0001-07, R.8012.19), and from both the "3D nano-architecturing of 2D crystals" (ARC 16/21-077) and the "Dynamically reconfigurable Moiré Materials" (ARC 21/26-116) projects. This research was also supported by a public grant overseen by the French National Research Agency (ANR) as part of the "Investissements d'Avenir" program Labex NanoSaclay (ANR-10-LABX-0035). It was also supported by the Mairie de Paris under the Emergence program with the "2DSPIN" project.

Conflict of Interest

The authors declare no conflict of interest.

Keywords

carbon nanotubes, graphene, molecules, quantum transport, spinterface, spintronics

Received: December 26, 2021
Revised: March 2, 2022
Published online:

[1] A. Fert, *Rev. Mod. Phys.* **2008**, *80*, 1517.
[2] P. A. Grünberg, *Rev. Mod. Phys.* **2008**, *80*, 1531.
[3] M. N. Baibich, J. M. Broto, A. Fert, F. N. Van Dau, F. Petroff, P. Etienne, G. Creuzet, A. Friederich, J. Chazelas, *Phys. Rev. Lett.* **1988**, *61*, 2472.
[4] G. Binasch, P. Grünberg, F. Saurenbach, W. Zinn, *Phys. Rev. B* **1989**, *39*, 4828.
[5] C. Day, *Phys. Today* **2007**, *60*, 12.
[6] B. Dieny, I. L. Prejbeanu, K. Garello, P. Gambardella, P. Freitas, R. Lehndorff, W. Raberg, U. Ebels, S. O. Demokritov, J. Akerman, A. Deac, P. Pirro, C. Adelmann, A. Anane, A. V. Chumak, A. Hirohata, S. Mangin, S. O. Valenzuela, M. C. Onbaşlı, M. D'Aquino, G. Prenat, G. Finocchio, L. Lopez-Diaz, R. Chantrell, O. Chubykalo-Fesenko, P. Bortolotti, *Nat. Electron.* **2020**, *3*, 446.
[7] P. Barla, V. K. Joshi, S. Bhat, *J. Comput. Electron.* **2021**, *20*, 805.
[8] M. G. Mankalale, S. S. Sapatnekar, *ACM J. Emerging Technol. Comput. Syst.* **2016**, *13*, 21.
[9] J. Grollier, D. Querlioz, K. Y. Camsari, K. Everschor-Sitte, S. Fukami, M. D. Stiles, *Nat. Electron.* **2020**, *3*, 360.
[10] J. Zhou, J. Chen, *Adv. Electron. Mater.* **2021**, *7*, 2100465.
[11] X. Li, J. Yang, *Natl. Sci. Rev.* **2016**, *3*, 365.
[12] A. Avsar, H. Ochoa, F. Guinea, B. Ozyilmaz, B. J. van Wees, I. J. Vera-Marun, *Rev. Mod. Phys.* **2019**, *92*, 021003.
[13] M. Galbiati, S. Tatay, C. Barraud, V. A. Dediu, F. Petroff, R. Mattana, P. Seneor, *MRS Bull.* **2014**, *39*, 602.
[14] P. Seneor, B. Dlubak, M.-B. Martin, A. Anane, H. Jaffres, A. Fert, *MRS Bull.* **2012**, *37*, 1245.
[15] J. Puebla, J. Kim, K. Kondou, Y. Otani, *Commun. Mater.* **2020**, *1*, 24.
[16] B. Behin-Aein, D. Datta, S. Salahuddin, S. Datta, *Nat. Nanotechnol.* **2010**, *5*, 266.
[17] J. Fabian, S. Das Sarma, *J. Vac. Sci. Technol., B: Microelectron. Nanometer Struct.* **1999**, *17*, 1708.
[18] S. Sanvito, A. R. Rocha, *J. Comput. Theor. Nanosci.* **2006**, *3*, 624.
[19] G. Schmidt, D. Ferrand, L. Molenkamp, A. Filip, B. van Wees, *Phys. Rev. B* **2000**, *62*, R4790.
[20] G. Schmidt, L. W. Molenkamp, *Semicond. Sci. Technol.* **2002**, *17*, 310.
[21] A. Fert, J. M. George, H. Jaffrès, R. Mattana, *IEEE Trans. Electron Devices* **2007**, *54*, 921.
[22] A. Fert, H. Jaffrès, *Phys. Rev. B* **2001**, *64*, 184420.
[23] S. Iijima, *Nature* **1991**, *354*, 56.
[24] K. S. Novoselov, A. K. Geim, S. V. Morozov, D. Jiang, Y. Zhang, S. V. Dubonos, I. V. Grigorieva, A. A. Firsov, *Science* **2004**, *306*, 666.
[25] Y. Cao, V. Fatemi, S. Fang, K. Watanabe, T. Taniguchi, E. Kaxiras, P. Jarillo-Herrero, *Nature* **2018**, *556*, 43.
[26] Y. Cao, J. M. Park, K. Watanabe, T. Taniguchi, P. Jarillo-Herrero, *Nature* **2021**, *595*, 526.
[27] A. L. Sharpe, E. J. Fox, A. W. Barnard, J. Finney, K. Watanabe, T. Taniguchi, M. A. Kastner, D. Goldhaber-Gordon, *Science* **2019**, *365*, 605.
[28] X. He, H. Htoon, S. K. Doorn, W. H. P. Pernice, F. Pyatkov, R. Krupke, A. Jeantet, Y. Chassagneux, C. Voisin, *Nat. Mater.* **2018**, *17*, 663.
[29] R. Bonnet, A. Lherbier, C. Barraud, M. L. Della Rocca, P. Lafarge, J.-C. Charlier, *Sci. Rep.* **2016**, *6*, 19701.
[30] M. Koshino, P. Moon, Y.-W. Son, *Phys. Rev. B* **2015**, *91*, 035405.
[31] O. E. Kwon, J.-W. Shin, H. Oh, C. Kang, H. Cho, B.-H. Kwon, C.-W. Byun, J.-H. Yang, K. Me Lee, J.-H. Han, N. Sung Cho, J. Hyuk Yoon, S. Jin Chae, J. Sung Park, H. Lee, C.-S. Hwang, J. Moon, J.-I. Lee, *J. Inf. Disp.* **2020**, *21*, 49.
[32] J.-C. C. Charlier, X. Blase, S. Roche, *Rev. Mod. Phys.* **2007**, *79*, 677.
[33] A. H. Castro Neto, F. Guinea, N. M. R. R. Peres, K. S. Novoselov, A. K. Geim, *Rev. Mod. Phys.* **2009**, *81*, 109.
[34] S. Yamashita, *APL Photonics* **2018**, *4*, 034301.
[35] V. I. Krinichnyi, S. D. Chemerisov, Y. S. Lebedev, **1997**, *55*, 16233.
[36] C. B. Harris, R. L. Schlupp, H. Schuch, *Phys. Rev. Lett.* **1973**, *30*, 1019.
[37] G. Feher, A. F. Kip, *Phys. Rev.* **1955**, *98*, 337.
[38] L. Banszerus, M. Schmitz, S. Engels, M. Goldsche, K. Watanabe, T. Taniguchi, B. Beschoten, C. Stampfer, *Nano Lett.* **2016**, *16*, 1387.
[39] D. Gall, *J. Appl. Phys.* **2016**, *119*, 085101.
[40] D. Huertas-Hernando, F. Guinea, A. Brataas, *Phys. Rev. B* **2006**, *74*, 155426.
[41] J. S. Moodera, G. Mathon, *J. Magn. Magn. Mater.* **1999**, *200*, 248.
[42] M. Beth Stearns, *J. Magn. Magn. Mater.* **1977**, *5*, 167.
[43] W. H. Kim, *Proc. IEEE* **1964**, *52*, 111.
[44] J. Mathon, *Phys. Rev. B* **1997**, *56*, 11810.
[45] R. Meservey, P. M. Tedrow, *Spin-Polarized Electron Tunneling*, North-Holland, Amsterdam, Netherlands**1994**.
[46] S. S. P. Parkin, C. Kaiser, A. Panchula, P. M. Rice, B. Hughes, M. Samant, S. H. Yang, *Nat. Mater.* **2004**, *3*, 862.

[47] A. R. Botello-Méndez, S. M. M. Dubois, A. Lherbier, J. C. Charlier, *Acc. Chem. Res.* **2014**, *47*, 3292.
[48] M. K. Horton, J. H. Montoya, M. Liu, K. A. Persson, *npj Comput. Mater.* **2019**, *5*, 64.
[49] P. Mavropoulos, N. Papanikolaou, P. H. Dederichs, *Phys. Rev. Lett.* **2000**, *85*, 1088.
[50] R. Kubo, *J. Phys. Soc. Jpn.* **1957**, *12*, 570.
[51] V. M. Karpan, P. A. Khomyakov, G. Giovannetti, A. A. Starikov, P. J. Kelly, *Phys. Rev. B* **2011**, *84*, 153406.
[52] V. M. Karpan, P. A. Khomyakov, A. A. Starikov, G. Giovannetti, M. Zwierzycki, M. Talanana, G. Brocks, J. Van Den Brink, P. J. Kelly, *Phys. Rev. B: Condens. Matter Mater. Phys.* **2008**, *78*, 195419.
[53] V. M. Karpan, G. Giovannetti, P. A. Khomyakov, M. Talanana, A. A. Starikov, M. Zwierzycki, J. van den Brink, G. Brocks, P. J. Kelly, *Phys. Rev. Lett.* **2007**, *99*, 176602.
[54] H. Haug, A.-P. Pauho, *Quantum Kinetics in Transport and Optics of Semiconductors*, Springer, Berlin **2008**.
[55] N. Jutong, I. Rungger, C. Schuster, U. Eckern, S. Sanvito, U. Schwingenschlögl, *Phys. Rev. B* **2012**, *86*, 205310.
[56] K. K. Saha, A. Blom, K. S. Thygesen, B. K. Nikolić, *Phys. Rev. B* **2012**, *85*, 184426.
[57] A. Hashmi, K. Nakanishi, T. Ono, *J. Phys. Soc. Jpn.* **2020**, *89*, 034708.
[58] M. Johnson, R. H. Silsbee, *Phys. Rev. Lett.* **1985**, *55*, 1790.
[59] M. Johnson, R. H. Silsbee, *Phys. Rev. B* **1988**, *37*, 5326.
[60] A. Hirohata, K. Yamada, Y. Nakatani, L. Prejbeanu, B. Diény, P. Pirro, B. Hillebrands, *J. Magn. Magn. Mater.* **2020**, *509*, 166711.
[61] T. Valet, A. Fert, *Phys. Rev. B* **1993**, *48*, 7099.
[62] H. Jaffrès, J.-M. George, A. Fert, *Phys. Rev. B* **2010**, *82*, 140408.
[63] C. Gould, C. Rüster, T. Jungwirth, E. Girgis, G. M. Schott, R. Giraud, K. Brunner, G. Schmidt, L. W. Molenkamp, *Phys. Rev. Lett.* **2004**, *93*, 117203.
[64] C. Schönenberger, A. Bachtold, C. Strunk, J.-P. Salvetat, L. Forró, *Appl. Phys. A: Mater. Sci. Process.* **1999**, *69*, 283.
[65] S. J. van der Molen, N. Tombros, B. J. van Wees, *Phys. Rev. B* **2006**, *73*, 220406.
[66] M. Drögeler, C. Franzen, F. Volmer, T. Pohlmann, L. Banszerus, M. Wolter, K. Watanabe, T. Taniguchi, C. Stampfer, B. Beschoten, *Nano Lett.* **2016**, *16*, 3533.
[67] P. J. Zomer, M. H. D. Guimarães, N. Tombros, B. J. van Wees, *Phys. Rev. B* **2012**, *86*, 161416.
[68] N. Tombros, C. Jozsa, M. Popinciuc, H. T. Jonkman, B. J. Van Wees, *Nature* **2007**, *448*, 571.
[69] J. Ingla-Aynés, R. J. Meijerink, B. J. V. Wees, *Nano Lett.* **2016**, *16*, 4825.
[70] Z. M. Gebeyehu, S. Parui, J. F. Sierra, M. Timmermans, M. J. Esplandiu, S. Brems, C. Huyghebaert, K. Garello, M. V. Costache, S. O. Valenzuela, *2D Mater.* **2019**, *6*, 034003.
[71] I. J. Vera-Marun, P. J. Zomer, a. Veligura, M. H. D. Guimarães, L. Visser, N. Tombros, H. J. van Elferen, U. Zeitler, B. J. van Wees, *Appl. Phys. Lett.* **2013**, *102*, 013106.
[72] M. H. D. Guimarães, P. J. Zomer, I. J. Vera-Marun, B. J. van Wees, *Nano Lett.* **2014**, *14*, 2952.
[73] A. Börjesson, W. Zhu, H. Amara, C. Bichara, K. Bolton, *Nano Lett.* **2009**, *9*, 1117.
[74] V. Vitale, A. Curioni, W. Andreoni, *J. Am. Chem. Soc.* **2008**, *130*, 5848.
[75] S. C. Lim, J. H. Jang, D. J. Bae, G. H. Han, S. Lee, I.-S. S. Yeo, Y. H. Lee, *Appl. Phys. Lett.* **2009**, *95*, 264103.
[76] J. Svensson, E. E. B. B. Campbell, *J. Appl. Phys.* **2011**, *110*, 111101.
[77] Y. He, J. Zhang, S. Hou, Y. Wang, Z. Yu, *Appl. Phys. Lett.* **2009**, *94*, 093107.
[78] D. Preusche, S. Schmidmeier, E. Pallecchi, C. Dietrich, A. K. Hüttel, J. Zweck, C. Strunk, *J. Appl. Phys.* **2009**, *106*, 084314.
[79] R. Bonnet, C. Barraud, P. Martin, M. L. Della Rocca, P. Lafarge, *Appl. Phys. Lett.* **2016**, *109*, 143110.
[80] K. Tsukagoshi, B. W. Alphenaar, H. Ago, *Nature* **1999**, *401*, 572.
[81] P. M. Tedrow, R. Meservey, *Phys. Rev. B* **1973**, *7*, 318.
[82] B. W. Alphenaar, K. Tsukagoshi, M. Wagner, *J. Appl. Phys.* **2001**, *89*, 6863.
[83] B. Zhao, I. Mönch, H. Vinzelberg, T. Mühl, C. M. Schneider, *Appl. Phys. Lett.* **2002**, *80*, 3144.
[84] J.-F. Dayen, T. L. Wade, M. Konczykowski, J.-E. Wegrowe, X. Hoffer, *Phys. Rev. B* **2005**, *72*, 073402.
[85] J. R. Kim, H. M. So, J.-J. Kim, J. Kim, *Phys. Rev. B* **2002**, *66*, 233401.
[86] P. E. Lindelof, J. Borggreen, A. Jensen, J. Nygard, P. R. Poulsen, *Phys. Scr.* **2002**, *T102*, 22.
[87] F. Pei, E. A. Laird, G. A. Steele, L. P. Kouwenhoven, *Nat. Nanotechnol.* **2012**, *7*, 630.
[88] K. Y. Wang, A. M. Blackburn, H. F. Wang, J. Wunderlich, D. A. Williams, *Appl. Phys. Lett.* **2013**, *102*, 093508.
[89] J. R. Hauptmann, J. Paaske, P. E. Lindelof, *Nat. Phys.* **2008**, *4*, 373.
[90] T. S. Jespersen, K. Grove-Rasmussen, J. Paaske, K. Muraki, T. Fujisawa, J. Nygård, K. Flensberg, *Nat. Phys.* **2011**, *7*, 348.
[91] S. Sahoo, T. Kontos, J. Furer, C. Hoffmann, M. Gräber, A. Cottet, C. Schönenberger, *Nat. Phys.* **2005**, *1*, 99.
[92] H. T. Man, I. J. W. Wever, A. F. Morpurgo, *Phys. Rev. B* **2006**, *73*, 241401.
[93] S. Sapmaz, P. Jarillo-Herrero, L. P. Kouwenhoven, H. S. J. van der Zant, *Semicond. Sci. Technol.* **2006**, *21*, S52.
[94] E. A. Laird, F. Kuemmeth, G. A. Steele, K. Grove-Rasmussen, J. Nygård, K. Flensberg, L. P. Kouwenhoven, *Rev. Mod. Phys.* **2015**, *87*, 703.
[95] A. Cottet, T. Kontos, S. Sahoo, H. T. Man, M.-S. Choi, W. Belzig, C. Bruder, A. F. Morpurgo, C. Schönenberger, *Semicond. Sci. Technol.* **2006**, *21*, S78.
[96] J. Samm, J. Gramich, A. Baumgartner, M. Weiss, C. Schönenberger, *J. Appl. Phys.* **2014**, *115*, 174309.
[97] Y. G. Semenov, K. W. Kim, G. J. Iafrate, *Phys. Rev. B* **2007**, *75*, 045429.
[98] L. E. Hueso, J. M. Pruneda, V. Ferrari, G. Burnell, J. P. Valdés-Herrera, B. D. Simons, P. B. Littlewood, E. Artacho, A. Fert, N. D. Mathur, *Nature* **2007**, *445*, 410.
[99] M. Bowen, M. Bibes, A. Barthélémy, J. P. Contour, A. Anane, Y. Lemaître, A. Fert, *Appl. Phys. Lett.* **2003**, *82*, 233.
[100] V. Garcia, M. Bibes, A. Barthélémy, M. Bowen, E. Jacquet, J.-P. Contour, A. Fert, *Phys. Rev. B* **2004**, *69*, 052403.
[101] C. Morgan, M. Misiorny, D. Metten, S. Heedt, T. Schäpers, C. M. Schneider, C. Meyer, *Phys. Rev. Appl.* **2016**, *5*, 054010.
[102] C. Morgan, C. M. Schneider, C. Meyer, *J. Appl. Phys.* **2012**, *111*, 07B309.
[103] C. Morgan, D. Metten, C. M. Schneider, C. Meyer, *Phys. Status Solidi* **2013**, *250*, 2622.
[104] F. J. Jedema, M. V. Costache, H. B. Heersche, J. J. A. Baselmans, B. J. van Wees, *Appl. Phys. Lett.* **2002**, *81*, 5162.
[105] H. Idzuchi, A. Fert, Y. Otani, *Phys. Rev. B* **2015**, *91*, 241407.
[106] C. Feuillet-Palma, T. Delattre, P. Morfin, J.-M. Berroir, G. Fève, D. C. Glattli, B. Plaçais, A. Cottet, T. Kontos, *Phys. Rev. B* **2010**, *81*, 115414.
[107] K. S. Novoselov, D. Jiang, F. Schedin, T. J. Booth, V. V. Khotkevich, S. V. Morozov, A. K. Geim, *Proc. Natl. Acad. Sci. U. S. A.* **2005**, *102*, 10451.
[108] F. J. Jedema, H. B. Heersche, A. T. Filip, J. J. A. A. Baselmans, B. J. Van Wees, *Nature* **2002**, *416*, 713.
[109] S. P. Dash, S. Sharma, R. S. Patel, M. P. de Jong, R. Jansen, *Nature* **2009**, *462*, 491.
[110] O. M. J. van 't Erve, A. T. Hanbicki, M. Holub, C. H. Li, C. Awo-Affouda, P. E. Thompson, B. T. Jonker, O. M. J. Van 'T Erve, A. T. Hanbicki, M. Holub, C. H. Li, C. Awo-Affouda, P. E. Thompson, B. T. Jonker, *Appl. Phys. Lett.* **2007**, *91*, 212109.

[111] X. Lou, C. Adelmann, S. A. Crooker, E. S. Garlid, J. Zhang, K. S. M. Reddy, S. D. Flexner, C. J. Palmstrøm, P. A. Crowell, *Nat. Phys.* **2007**, *3*, 197.
[112] E. W. Hill, A. K. Geim, K. Novoselov, F. Schedin, P. Blake, *IEEE Trans. Magn.* **2006**, *42*, 2694.
[113] M. Popinciuc, C. Józsa, P. J. Zomer, N. Tombros, A. Veligura, H. T. Jonkman, B. J. van Wees, *Phys. Rev. B* **2009**, *80*, 214427.
[114] W. Han, K. Pi, K. M. McCreary, Y. Li, J. J. I. Wong, A. G. Swartz, R. K. Kawakami, *Phys. Rev. Lett.* **2010**, *105*, 167202.
[115] S. Roche, J. Åkerman, B. Beschoten, J.-C. C. Charlier, M. Chshiev, S. P. Dash, B. Dlubak, J. Fabian, A. Fert, M. Guimarães, F. Guinea, I. Grigorieva, C. Schönenberger, P. Seneor, C. Stampfer, S. O. Valenzuela, X. Waintal, B. Van Wees, S. Prasad Dash, B. Dlubak, J. Fabian, A. Fert, M. Guimarães, F. Guinea, I. Grigorieva, C. Schönenberger, P. Seneor, C. Stampfer, S. O. Valenzuela, X. Waintal, et al., *2D Mater.* **2015**, *2*, 030202.
[116] M. H. D. Guimarães, P. J. Zomer, J. Ingla-Aynés, J. C. Brant, N. Tombros, B. J. Van Wees, *Phys. Rev. Lett.* **2014**, *113*, 086602.
[117] J. Ingla-Aynés, M. H. D. Guimarães, R. J. Meijerink, P. J. Zomer, B. J. Van Wees, *Phys. Rev. B* **2015**, *92*, 201410.
[118] W. Yan, L. C. Phillips, M. Barbone, S. J. Hämäläinen, A. Lombardo, M. Ghidini, X. Moya, F. MacCherozzi, S. Van Dijken, S. S. Dhesi, A. C. Ferrari, N. D. Mathur, *Phys. Rev. Lett.* **2016**, *117*, 147201.
[119] E. Fourneau, A. V. Silhanek, N. D. Nguyen, *Phys. Rev. Appl.* **2021**, *15*, 034058.
[120] M. Cosset-Chéneau, L. Vila, G. Zahnd, D. Gusakova, V. T. Pham, C. Grèzes, X. Waintal, A. Marty, H. Jaffrès, J. P. Attané, *Phys. Rev. Lett.* **2021**, *126*, 027201.
[121] E. Fourneau, A. V. Silhanek, N. D. Nguyen, *Phys. Rev. Appl.* **2020**, *14*, 024020.
[122] W. Han, K. M. McCreary, K. Pi, W. H. Wang, Y. Li, H. Wen, J. R. Chen, R. K. Kawakami, *J. Magn. Magn. Mater.* **2012**, *324*, 369.
[123] B. Dlubak, M.-B. B. Martin, C. Deranlot, B. Servet, S. Xavier, R. Mattana, M. Sprinkle, C. Berger, W. A. De Heer, F. Petroff, A. Anane, P. Seneor, A. Fert, *Nat. Phys.* **2012**, *8*, 557.
[124] M. Piquemal-Banci, R. Galceran, S. M.-M. Dubois, V. Zatko, M. Galbiati, F. Godel, M.-B. Martin, R. S. Weatherup, F. Petroff, A. Fert, J.-C. Charlier, J. Robertson, S. Hofmann, B. Dlubak, P. Seneor, *Nat. Commun.* **2020**, *11*, 5670.
[125] B. Dlubak, P. Seneor, A. Anane, C. Barraud, C. Deranlot, D. Deneuve, B. Servet, R. Mattana, F. Petroff, A. Fert, *Appl. Phys. Lett.* **2010**, *97*, 092502.
[126] M. V. Kamalakar, C. Groenveld, A. Dankert, S. P. Dash, *Nat. Commun.* **2015**, *6*, 6766.
[127] M. Piquemal-Banci, R. Galceran, S. Caneva, M. B. Martin, R. S. Weatherup, P. R. Kidambi, K. Bouzehouane, S. Xavier, A. Anane, F. Petroff, A. Fert, J. Robertson, S. Hofmann, B. Dlubak, P. Seneor, *Appl. Phys. Lett.* **2016**, *108*, 102404.
[128] M. Piquemal-Banci, R. Galceran, F. Godel, S. Caneva, M. B. Martin, R. S. Weatherup, P. R. Kidambi, K. Bouzehouane, S. Xavier, A. Anane, F. Petroff, A. Fert, S. M. M. Dubois, J. C. Charlier, J. Robertson, S. Hofmann, B. Dlubak, P. Seneor, *ACS Nano* **2018**, *12*, 4712.
[129] J.-G. (Jimmy) Zhu, C. Park, *Mater. Today* **2006**, *9*, 36.
[130] M. B. Martin, B. Dlubak, R. S. Weatherup, H. Yang, C. Deranlot, K. Bouzehouane, F. F. F. Petroff, A. Anane, S. Hofmann, J. Robertson, A. Fert, P. Seneor, *ACS Nano* **2014**, *8*, 7890.
[131] M. Galbiati, V. Zatko, F. Godel, P. Hirschauer, A. Vecchiola, K. Bouzehouane, S. Collin, B. Servet, A. Cantarero, F. Petroff, M. B. Martin, B. Dlubak, P. Seneor, *ACS Appl. Electron. Mater.* **2020**, *2*, 3508.
[132] L. M. Kern, R. Galceran, V. Zatko, M. Galbiati, F. Godel, D. Perconte, F. Bouamrane, E. Gaufrès, A. Loiseau, P. Brus, O. Bezencenet, M. B. Martin, B. Servet, F. Petroff, B. Dlubak, P. Seneor, *Appl. Phys. Lett.* **2019**, *114*, 053107.
[133] D. B. Farmer, R. G. Gordon, *Nano Lett.* **2006**, *6*, 699.
[134] N. Chiodarelli, A. Delabie, S. Masahito, Y. Kashiwagi, O. Richard, H. Bender, D. J. Cott, M. Heyns, S. De Gendt, G. Groeseneken, P. M. Vereecken, *MRS Online Proc. Libr.* **2011**, *1283*, 46.
[135] F. V. Ferreira, L. D. S. Cividanes, F. S. Brito, B. R. C. de Menezes, W. Franceschi, E. A. N. Simonetti, G. P. Thim, in *SpringerBriefs Appl. Sci. Technol.*, Springer Verlag, **2016**, pp. 1–29.
[136] S. Mallakpour, S. Soltanian, *RSC Adv.* **2016**, *6*, 109916.
[137] X. Peng, S. S. Wong, *Adv. Mater.* **2009**, *21*, 625.
[138] D. Cahen, A. Kahn, E. Umbach, *Mater. Today* **2005**, *8*, 32.
[139] H. Ishii, K. Sugiyama, E. Ito, K. Seki, *Adv. Mater.* **1999**, *11*, 605.
[140] T.-C. Tseng, C. Urban, Y. Wang, R. Otero, S. L. Tait, M. Alcamí, D. Écija, M. Trelka, J. M. Gallego, N. Lin, M. Konuma, U. Starke, A. Nefedov, A. Langner, C. Wöll, M. Á. Herranz, F. Martín, N. Martín, K. Kern, R. Miranda, *Nat. Chem.* **2010**, *2*, 374.
[141] C. Barraud, P. Seneor, R. Mattana, S. Fusil, K. Bouzehouane, C. Deranlot, P. Graziosi, L. Hueso, I. Bergenti, V. Dediu, F. Petroff, A. Fert, *Nat. Phys.* **2010**, *6*, 615.
[142] S. Sanvito, *Nature* **2010**, *467*, 664.
[143] S. Sanvito, *Nat. Phys.* **2010**, *6*, 562.
[144] A. R. Rocha, V. M. García-Suárez, S. W. Bailey, C. J. Lambert, J. Ferrer, S. Sanvito, *Nat. Mater.* **2005**, *4*, 335.
[145] Z. H. Xiong, D. Wu, Z. V. Vardeny, J. Shi, *Nature* **2004**, *427*, 821.
[146] T. S. Santos, J. S. Lee, P. Migdal, I. C. Lekshmi, B. Satpati, J. S. Moodera, *Phys. Rev. Lett.* **2007**, *98*, 016601.
[147] S. Delprat, M. Galbiati, S. Tatay, B. Quinard, C. Barraud, F. Petroff, P. Seneor, R. Mattana, *J. Phys. D: Appl. Phys.* **2018**, *51*, 473001.
[148] A. Droghetti, P. Thielen, I. Rungger, N. Haag, N. Großmann, J. Stöckl, B. Stadtmüller, M. Aeschlimann, S. Sanvito, M. Cinchetti, *Nat. Commun.* **2016**, *7*, 12668.
[149] F. Djeghloul, M. Gruber, E. Urbain, D. Xenioti, L. Joly, S. Boukari, J. Arabski, H. Bulou, F. Scheurer, F. Bertran, P. Le Fèvre, A. Taleb-Ibrahimi, W. Wulfhekel, G. Garreau, S. Hajjar-Garreau, P. Wetzel, M. Alouani, E. Beaurepaire, M. Bowen, W. Weber, *J. Phys. Chem. Lett.* **2016**, *7*, 2310.
[150] A. Bedoya-Pinto, S. G. Miralles, S. Vélez, A. Atxabal, P. Gargiani, M. Valvidares, F. Casanova, E. Coronado, L. E. Hueso, *Adv. Funct. Mater.* **2018**, *28*, 1702099.
[151] H. Vasquez, R. Oszwaldowski, P. Pou, J. Ortega, F. Flores, A. Kahn, H. Vázquez, R. Oszwaldowski, P. Pou, J. Ortega, R. Pérez, F. Flores, A. Kahn, *Europhys. Lett.* **2004**, *65*, 802.
[152] A. Kahn, N. Koch, W. Gao, *J. Polym. Sci., Part B: Polym. Phys.* **2003**, *41*, 2529.
[153] J. S. Moodera, B. Koopmans, P. M. Oppeneer, *MRS Bull.* **2014**, *39*, 578.
[154] N. Atodiresei, K. V. Raman, *MRS Bull.* **2014**, *39*, 596.
[155] K. Katcko, E. Urbain, F. Ngassam, L. Kandpal, B. Chowrira, F. Schleicher, U. Halisdemir, D. Wang, T. Scherer, D. Mertz, B. Leconte, N. Beyer, D. Spor, P. Panissod, A. Boulard, J. Arabski, C. Kieber, E. Sternitzky, V. Da Costa, M. Hehn, F. Montaigne, A. Bahouka, W. Weber, E. Beaurepaire, C. Kübel, D. Lacour, M. Alouani, S. Boukari, M. Bowen, *Adv. Funct. Mater.* **2021**, *31*, 2009467.
[156] S. Javaid, M. Bowen, S. Boukari, L. Joly, J.-B. B. Beaufrand, X. Chen, Y. J. Dappe, F. Scheurer, J.-P. P. Kappler, J. Arabski, W. Wulfhekel, M. Alouani, E. Beaurepaire, *Phys. Rev. Lett.* **2010**, *105*, 077201.
[157] S. Schmaus, A. Bagrets, Y. Nahas, T. K. Yamada, A. Bork, M. Bowen, E. Beaurepaire, F. Evers, W. Wulfhekel, *Nat. Nanotechnol.* **2011**, *6*, 185.
[158] M. Gruber, F. Ibrahim, F. Djedhloul, C. Barraud, G. Garreau, S. Boukari, H. Isshiki, L. Joly, E. Urbain, M. Peter, M. Studniarek, V. Da Costa, H. Jabbar, H. Bulou, V. Davesne, U. Halisdemir, J. Chen, D. Xenioti, J. Arabski, K. Bouzehouane, C. Deranlot, S. Fusil, E. Otero, F. Choueikani, K. Chen, P. Ohresser, F. Bertran, P. Le Fèvre, A. Taleb-Ibrahimi, W. Wulfhekel, et al., *Proc. SPIE* **2016**, *9931*, 993130.

[159] C. Barraud, K. Bouzehouane, C. Deranlot, D. J. J. Kim, R. Rakshit, S. Shi, J. Arabski, M. Bowen, E. Beaurepaire, S. Boukari, F. Petroff, P. Seneor, R. Mattana, *Dalton Trans.* **2016**, *45*, 16694.
[160] C. Barraud, K. Bouzehouane, C. Deranlot, S. Fusil, H. Jabbar, J. Arabski, R. Rakshit, D.-J. J. Kim, C. Kieber, S. Boukari, M. Bowen, E. Beaurepaire, P. Seneor, R. Mattana, F. Petroff, *Phys. Rev. Lett.* **2015**, *114*, 206603.
[161] A. F. Takács, F. Witt, S. Schmaus, T. Balashov, M. Bowen, E. Beaurepaire, W. Wulfhekel, *Phys. Rev. B* **2008**, *78*, 233404.
[162] N. Atodiresei, J. Brede, P. Lazić, V. Caciuc, G. Hoffmann, R. Wiesendanger, S. Blügel, *Phys. Rev. Lett.* **2010**, *105*, 066601.
[163] T.-N. Lam, Y.-L. Lai, C.-H. Chen, P.-H. Chen, Y.-L. Chan, D.-H. Wei, H.-J. Lin, C. T. Chen, J.-H. Wang, J.-T. Sheu, Y.-J. Hsu, *Phys. Rev. B* **2015**, *91*, 041204.
[164] K. V. Raman, A. M. Kamerbeek, A. Mukherjee, N. Atodiresei, T. K. Sen, P. Lazić, V. Caciuc, R. Michel, D. Stalke, S. K. Mandal, S. Blügel, M. Münzenberg, J. S. Moodera, *Nature* **2013**, *493*, 509.
[165] Z. Zhang, S. Qiu, Y. Miao, J. Ren, C. Wang, G. Hu, *Appl. Surf. Sci.* **2017**, *409*, 60.
[166] D. Li, R. Banerjee, S. Mondal, I. Maliyov, M. Romanova, Y. J. Dappe, A. Smogunov, *Phys. Rev. B* **2019**, *99*, 115403.
[167] A. Smogunov, Y. J. Dappe, *Nano Lett.* **2015**, *15*, 3552.
[168] D. Li, Y. J. Dappe, A. Smogunov, *J. Phys. Condens. Matter* **2019**, *31*, 405301.
[169] J. Huang, K. Xu, S. Lei, H. Su, S. Yang, Q. Li, J. Yang, *J. Chem. Phys.* **2012**, *136*, 064707.
[170] H. Hao, X. H. Zheng, Z. X. Dai, Z. Zeng, *Appl. Phys. Lett.* **2010**, *96*, 192112.
[171] J. Zeng, K.-Q. Chen, *J. Mater. Chem. C* **2013**, *1*, 4014.
[172] J. Peng, W. X. Zhou, K. Q. Chen, *Phys. Lett. A* **2014**, *378*, 3126.
[173] M. Cinchetti, K. Heimer, J. P. Wüstenberg, O. Andreyev, M. Bauer, S. Lach, C. Ziegler, Y. Gao, M. Aeschlimann, *Nat. Mater.* **2009**, *8*, 115.
[174] K. Balasubramanian, M. Burghard, *Small* **2005**, *1*, 180.
[175] Y.-P. Sun, K. Fu, A. Yi Lin, W. Huang, *Acc. Chem. Res.* **2002**, *35*, 1096.
[176] S. B. Sinnott, *J. Nanosci. Nanotechnol.* **2002**, *2*, 113.
[177] D. Tasis, N. Tagmatarchis, A. Bianco, M. Prato, *Chem. Rev.* **2006**, *106*, 1105.
[178] V. Georgakilas, M. Otyepka, A. B. Bourlinos, V. Chandra, N. Kim, K. C. Kemp, P. Hobza, R. Zboril, K. S. Kim, *Chem. Rev.* **2012**, *112*, 6156.
[179] G. Bottari, M. Á. Herranz, L. Wibmer, M. Volland, L. Rodríguez-Pérez, D. M. Guldi, A. Hirsch, N. Martín, F. D'Souza, T. Torres, M. Ángeles Herranz, L. Wibmer, M. Volland, L. Rodríguez-Pérez, D. M. Guldi, A. Hirsch, N. Martín, F. D'Souza, T. Torres, *Chemical Functionalization and Characterization of Graphene-Based Materials*, The Royal Society Of Chemistry, Burlington House, London**2017**.
[180] J. Zhao, Z. Chen, Z. Zhou, H. Park, P. von R Schleyer, J. P. Lu, P. R. Von Schleyer, J. P. Lu, *ChemPhysChem* **2005**, *6*, 598.
[181] Z. Q. Zhang, B. Liu, Y. L. Chen, H. Jiang, K. C. Hwang, Y. Huang, *Nanotechnology* **2008**, *19*, 395702.
[182] T. Shiraki, Y. Miyauchi, K. Matsuda, N. Nakashima, *Acc. Chem. Res.* **2020**, *53*, 1846.
[183] P. A. Denis, F. Iribarne, *J. Phys. Chem. C* **2011**, *115*, 195.
[184] M. Gong, T. A. Shastry, Q. Cui, R. R. Kohlmeyer, K. A. Luck, A. Rowberg, T. J. Marks, M. F. Durstock, H. Zhao, M. C. Hersam, S. Ren, *ACS Appl. Mater. Interfaces* **2015**, *7*, 7428.
[185] J. Oh, S. Roh, W. Yi, H. Lee, J. Yoo, *J. Vac. Sci. Technol., B: Microelectron. Nanometer Struct.–Process., Meas., Phenom.* **2004**, *22*, 1416.
[186] P. J. Britto, K. S. V Santhanam, A. Rubio, J. A. Alonso, P. M. Ajayan, *Adv. Mater.* **1999**, *11*, 154.
[187] A. Matković, M. Kratzer, B. Kaufmann, J. Vujin, R. Gajić, C. Teichert, *Sci. Rep.* **2017**, *7*, 9544.
[188] W. Pei, T. Zhang, Y. Wang, Z. Chen, A. Umar, H. Li, W. Guo, *Nanoscale* **2017**, *9*, 16273.
[189] C. N. R. Rao, R. Voggu, *Mater. Today* **2010**, *13*, 34.
[190] T. Han, A. Nag, S. C. Mukhopadhyay, Y. Xu, *Sens. Actuators, A* **2019**, *291*, 107.
[191] W. Yuan, G. Shi, *J. Mater. Chem. A* **2013**, *1*, 10078.
[192] P. Bondavalli, *C. R. Phys.* **2010**, *11*, 389.
[193] J. Park, M. Yan, *Acc. Chem. Res.* **2013**, *46*, 181.
[194] A. Hirsch, J. M. Englert, F. Hauke, *Acc. Chem. Res.* **2013**, *46*, 87.
[195] J. Pinson, F. Podvorica, *Chem. Soc. Rev.* **2005**, *34*, 429.
[196] M. Delamar, R. Hitmi, J. Pinson, J. M. Saveant, *J. Am. Chem. Soc.* **1992**, *114*, 5883.
[197] M. Kurahashi, X. Sun, *J. Phys. Chem. Lett.* **2021**, *12*, 8489.
[198] J. L. Bahr, J. Yang, D. V. Kosynkin, M. J. Bronikowski, R. E. Smalley, J. M. Tour, *J. Am. Chem. Soc.* **2001**, *123*, 6536.
[199] C. Barraud, M. Lemaitre, R. Bonnet, J. Rastikian, C. Salhani, S. Lau, Q. van Nguyen, P. Decorse, J.-C. C. Lacroix, M. L. Della Rocca, P. Lafarge, P. Martin, *Nanoscale Adv.* **2019**, *1*, 414.
[200] H. Yan, A. J. Bergren, R. McCreery, M. L. Della Rocca, P. Martin, P. Lafarge, J.-C. C. Lacroix, M. L. Della Rocca, P. Martin, P. Lafarge, J.-C. Lacroix, *Proc. Natl. Acad. Sci. U. S. A.* **2013**, *110*, 5326.
[201] Q. V. Nguyen, P. Martin, D. Frath, M. L. Della Rocca, F. Lafolet, C. Barraud, P. Lafarge, V. Mukundan, D. James, R. L. McCreery, J.-C. Lacroix, *J. Am. Chem. Soc.* **2017**, *139*, 11913.
[202] P. Martin, M. L. Della Rocca, A. Anthore, P. Lafarge, J.-C. Lacroix, *J. Am. Chem. Soc.* **2012**, *134*, 154.
[203] J. C. Toscano-Figueroa, N. Natera-Cordero, D. A. Bandurin, C. R. Anderson, V. H. Guarochico-Moreira, I. V. Grigorieva, I. J. Vera-Marun, *Phys. Rev. Appl.* **2021**, *15*, 054018.
[204] D. Wang, C. Nordman, J. M. Daughton, Z. Qian, J. Fink, *IEEE Trans. Magn.* **2004**, *40*, 2269.
[205] A. Sugihara, K. Yakushiji, S. Yuasa, *Appl. Phys. Express* **2019**, *12*, 023002.
[206] W. Shen, D. Mazumdar, X. Zou, X. Liu, B. D. Schrag, G. Xiao, *Appl. Phys. Lett.* **2006**, *88*, 182508.
[207] A. L. Friedman, O. M. J. van 't Erve, J. T. Robinson, K. E. Whitener, B. T. Jonker, *ACS Nano* **2015**, *9*, 6747.
[208] A. L. Friedman, O. M. J. Van 'T Erve, C. H. Li, J. T. Robinson, B. T. Jonker, O. M. J. van 't Erve, C. H. Li, J. T. Robinson, B. T. Jonker, *Nat. Commun.* **2014**, *5*, 3161.
[209] D. Bouilly, J. Cabana, F. Meunier, M. Desjardins-Carrière, F. Lapointe, P. Gagnon, F. L. Larouche, E. Adam, M. Paillet, R. Martel, *ACS Nano* **2011**, *5*, 4927.
[210] D. Bouilly, J. L. Janssen, J. Cabana, M. Côté, R. Martel, *ACS Nano* **2015**, *9*, 2626.
[211] R. Bonnet, P. Martin, S. Suffit, P. Lafarge, A. Lherbier, J. C. Charlier, M. L. Della Rocca, C. Barraud, *Sci. Adv.* **2020**, *6*, eaba5494.

Pascal Martin completed his undergraduate studies in Marseille (france), before moving to the University of Bordeaux where he obtained a Ph.D. in organic chemistry in 2004. In 2007 he joined the ITODYS laboratory at University of Paris as an assistant professor, after having spent two successful years as a postdoctoral fellow at University of Tokyo (LIMMS, Japan) and at IM2NP (Toulon, France). His research interest are centered around the chemical functionalization based on self assembled and electrochemical processes.

Bruno Dlubak is a CNRS Researcher at the Unité Mixte de Physique CNRS-Thales lab, associated to the Paris-Saclay University. He received his Ph.D. from the University of Paris-Sud in 2011 working on graphene spintronics. After a postdoctoral appointment at the University of Cambridge working in John Robertson group, he became a CNRS Researcher in 2014. His current research interests concern the exploration of 2D materials for electronics and spintronics devices, with a focus on spin dependent transport and injection in nanostructures and 2D materials.

Pierre Seneor is professor at Université Paris-Saclay and Unité Mixte de Physique CNRS/Thales industrial/academic lab. He received his Ph.D. from Ecole Polytechnique in 2000 under the supervision of A. Fert working on spin dependent tunneling in oxides. After a post-doc at CALTECH, in 2003 he joined the physics department of University of Paris-Sud (now Paris-Saclay) in Orsay where he is now full professor. He was awarded Junior Fellow of the Institut Universitaire de France excellency institute. His current research interests include exploring the physics of novel molecular and 2D materials in low dimension towards nanoelectronics and spintronics devices.

Richard Mattana received his Ph.D. degree in materials science from the Université Paris-Sud (now Paris-Saclay) in Paris in 2003. His thesis research focused on spin-dependent transport through inorganic semiconductor nanostructures. Since 20404 he is a CNRS researcher at Unité Mixte de Physique CNRS/Thales (Palaiseau, France). His research activity is focused on spin transport through molecular materials.

Marie-Blandine Martin graduated from the Université Paris Diderot and Ecole Normale Supérieure de Lyon and received her Ph.D. from the University of Paris-Sud in 2015 working on spintronics with graphene. After a post-doctoral position at the University of Cambridge in Stephan Hofmann group, she is now working as a researcher in the Unité de Physique CNRS/Thales lab. Her research interests focus on the exploration of the exciting properties of 2D materials in electronics and spintronics devices.

Philippe Lafarge is professor of physics at Université de Paris. He received his Ph.D. in physics at the University Pierre et Marie Curie in 1993 working on Coulomb blockade. He spent two years at the university of Delft and then joined the industry of flat panel display. In 1997, he became an assistant professor at the University of Grenoble where he worked on superconducting quantum bits. He joined the Matériaux et Phénomènes Quantique laboratory at Université de Paris in 2003. His current interests are focused on the fundamental aspects of electronic, thermal and spin transport at the molecular scale.

François Mallet received his Ph.D. in fundamental physics on mesoscopic electronic transport from Grenoble Alpes University in 2006. After two post-doctorates in superconducting quantum circuits at CEA-Saclay and JILA-Colorado University, he became an associate professor at Sorbonne University in 2011. After a decade working on quantum information processing with Josephson junction circuits at Laboratoire de Physique de l'Ecole Normale Supérieure, he joined the Laboratory des Matériaux et Phénomènes Quantiques in 2020 to put his competences in microwave engineering into generation and detection of spin currents in 2D van der Waals materials.

Maria Luisa Della Rocca obtained her Ph. D. degree in physics from the University of Salerno (Italy) in 2004. Her Ph.D. research focused on proximity effect in superconductor/ferromagnetic junctions. She successively joined the SPEC at CEA-Saclay (France) working on quantum transport in superconductive atomic contacts. Since 2006 she is assistant professor in physics at the Université de Paris working in the Matériaux et Phénomènes Quantiques Laboratory. Her research is currently focused on charge, spin, and thermal transport in 2D material and hybrid organic/inorganic low dimensional systems.

Simon M.-M. Dubois completed his Ph.D. at UCLouvain (Belgium). His thesis focused on the description of electronic transport in nano-structures. In 2010, he joined the Cavendish Laboratory, University of Cambridge, to develop new electronic structure prediction algorithms. In 2015, he received an FNRS fellowship to investigate spintronics phenomena in 2D systems. In 2018, he joined the Unité mixte the physique CNRS/Thales working towards the introduction of 2D materials in magnetic tunnel junctions. He is currently research associate at UCLouvain. His research interests include the understanding of spin phenomena at interfaces and in low-dimensional systems.

Jean-Christophe Charlier is professor of physics at the Ecole Polytechnique of the University of Louvain in Belgium. He received his Ph.D. degree in applied physics in 1994 at UCLouvain. His main scientific interests are centered on theoretical condensed matter physics and nanosciences, covering the areas of ab initio electronic, structural and magnetic properties of nano-materials and spin-dependent quantum transport in reduced-dimensional solids such as nanotubes, graphene, and new 2D materials. The research objective consists in explaining or predicting the properties of these nanostructures using first-principles theories and computational physics.

Clément Barraud received his Ph.D. degree in physics from the Université Pierre et Marie Curie (now Sorbonne Université) in Paris in 2011. His thesis research focused on spin injection phenomena at ferromagnetic metal/molecules interfaces. He then joined ETH Zürich between 2011 and 2013 to study quantum transport in bilayer graphene-based devices. Since 2013 he is assistant professor in physics at the Université de Paris working in the Matériaux et Phénomènes Quantiques laboratory. His research interests are centered around quantum spintronics and more specifically around spin injection and transport phenomena through molecules and 2D materials.